NANO-SCALE CHARACTERIZATION OF ULK AND BEOL STRUCTURES: MODULUS MAPPING AND WEDGE INDENTATION ADHESION MEASUREMENTS

Kong Boon Yeap, Christoph Sander,
Malgorzata Kopycinska-Müller,
Martin Gall,
Ehrenfried Zschech

Fraunhofer IZFP Dresden, Germany

Lei Chen

Institute of High Performance Computing, Singapore

Marco Jungmann, Reinhard Krause-Rehberg

Martin Luther Universität Halle, Germany

Sukesh Mahajan

SBA Materials, USA

Outline

- Motivation
- Nanoindentation and FE simulation on **different pore topology** of OSG (organosilicate glass)
- Measurement of the effective **CTE** of BEoL structure
- Wedge-Indentation on **SA-OSG** (self-assembled OSG)
- Conclusion

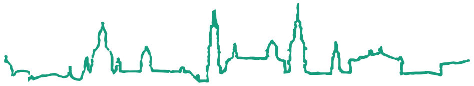

multi-scale database

MOTIVATION

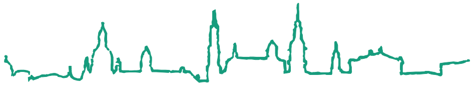

3D TSV scheme

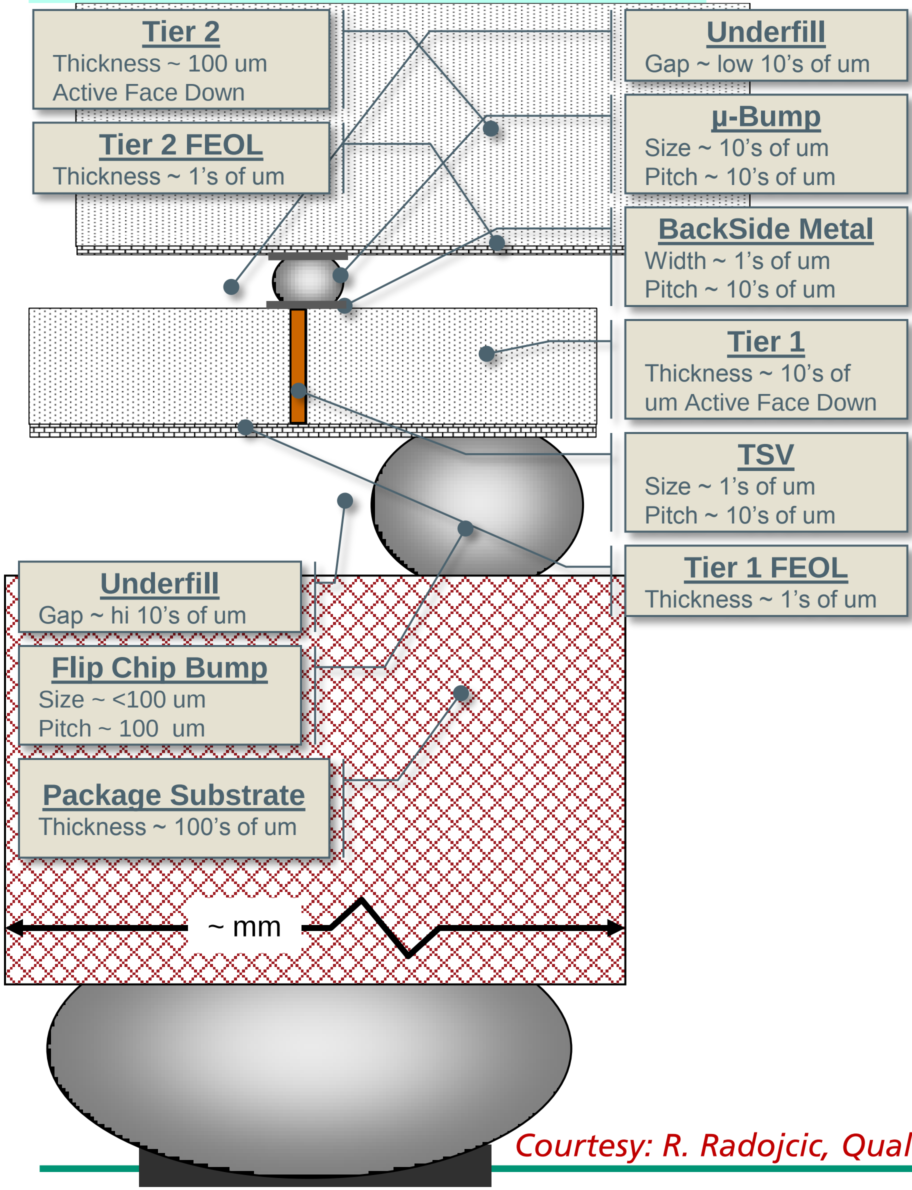

Courtesy: R. Radojcic, Qualcomm

Integrated Heterogeneous 2-Die Stack

- Tier 1 : CMOS Logic SoC
  - **TSV (connect frontside to backside)**
  - Very thin Wafer (manage TSV aspect ratio)
  - Active face down incl. **BEoL**
- Interface µ-Bump
  - Backside RDL Metal (interface to µ-Bump and/or routing to allow offset of µ-Bump vs TSV)
  - **µ-Bump (Tier to Tier interconnect)**
  - Very thin underfill
- Tier 2 : Commercial Die
  - Memory or Analog die, or…
  - Frontside Metal (interface to µ-Bump)
  - Active face down & Pretty Thin
- Flip Chip (C4) Bump
  - Regular flip chip bump
  - Regular underfill
- Package
  - Regular PCB substrate
  - Regular plastic molding
  - Regular Package BGA Bump

Studied 3D IC

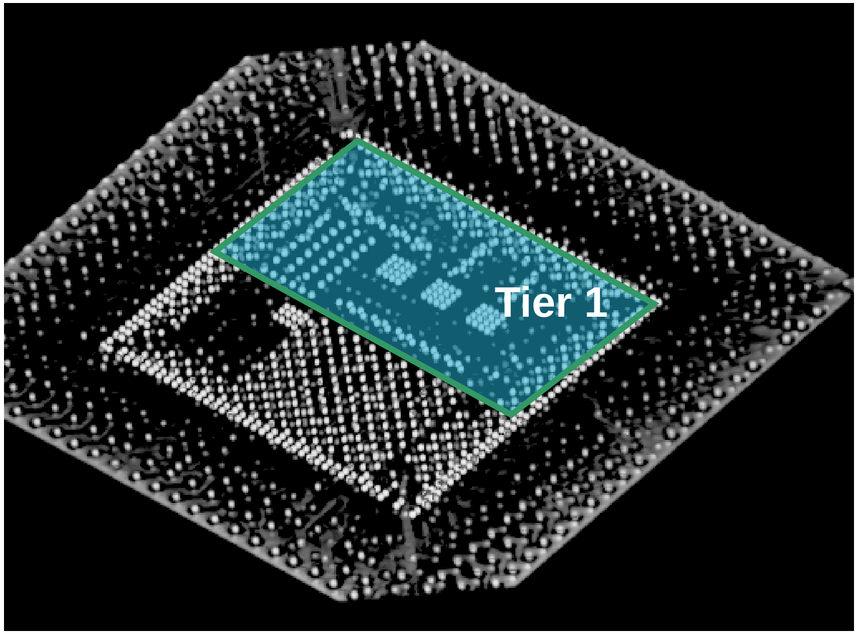

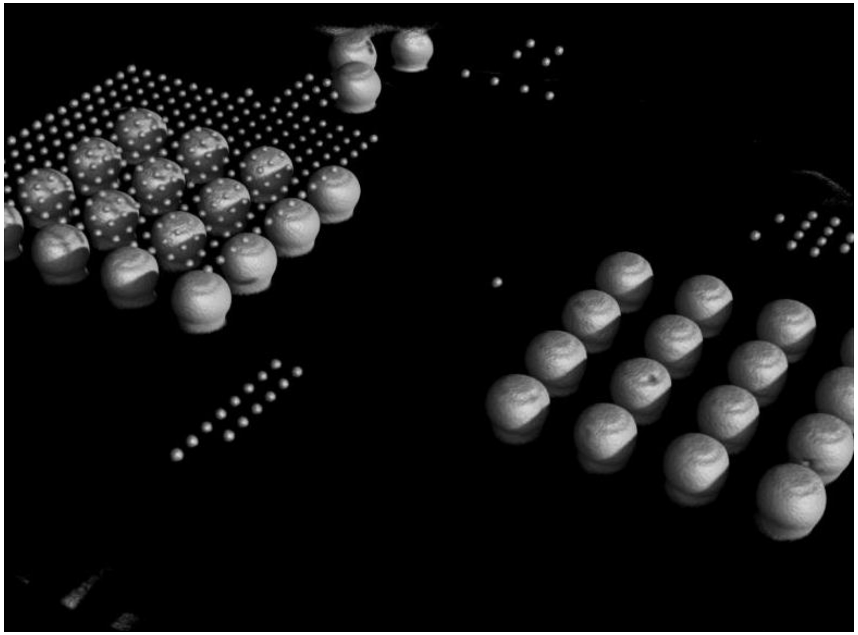

Micro-XCT Courtesy: Peter Krüger

- Young’s modulus – Nanoindentation
- CTE – Coefficient of Thermal Expansion
- Adhesion of Ultra Low K on Silicon – Wedge Indentation

Stress engineering in 3D IC structures: Need of database and input for database: Multi-scale materials data

Stress-related phenomena caused by 3D TSV integration influence:

- chip performance (and variability),
- yield and reliability.

Stress **management** in complex systems requires:

- multi-scale modeling, including accurate MULTI-SCALE MATERIALS DATA
- Input data for simulation
- Model validation (and calibration)

➔ Multi-scale materials database concept [1]

Multi-scale Materials Characterization needed

- Multi-scale (thermo-)mechanical materials data

---

[1] V. Sukharev, E. Zschech, Int. Workshop "Stress Management for 3D ICs using Through Silicon Vias", Albany/NY 2010, AIP Proc. 1378, pp. 21 – 49 (2011)

Young’s Modulus

NANO-INDENTATION TECHNIQUE

Motivation

Relations between mechanical properties and structure at micro- and nano-scale:

- Optimum pore/molecular structure (CPI and dielectric reliability)
- Enable a physics-based IC design

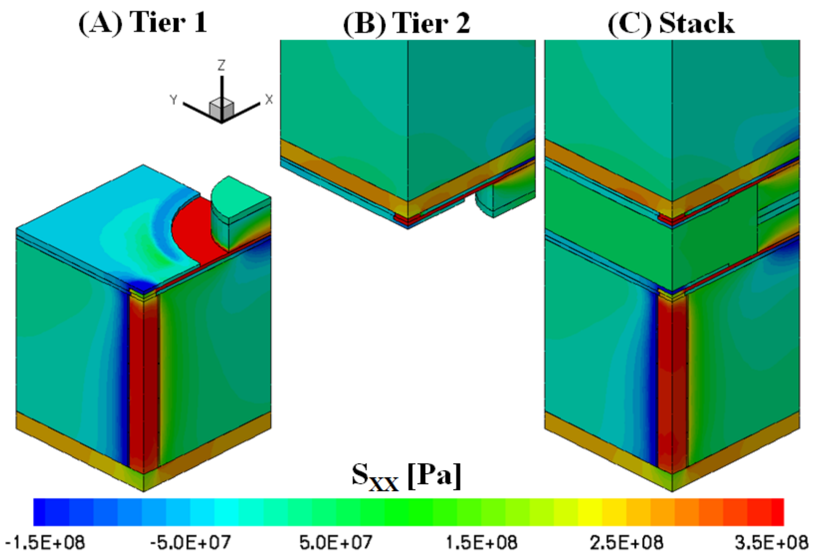

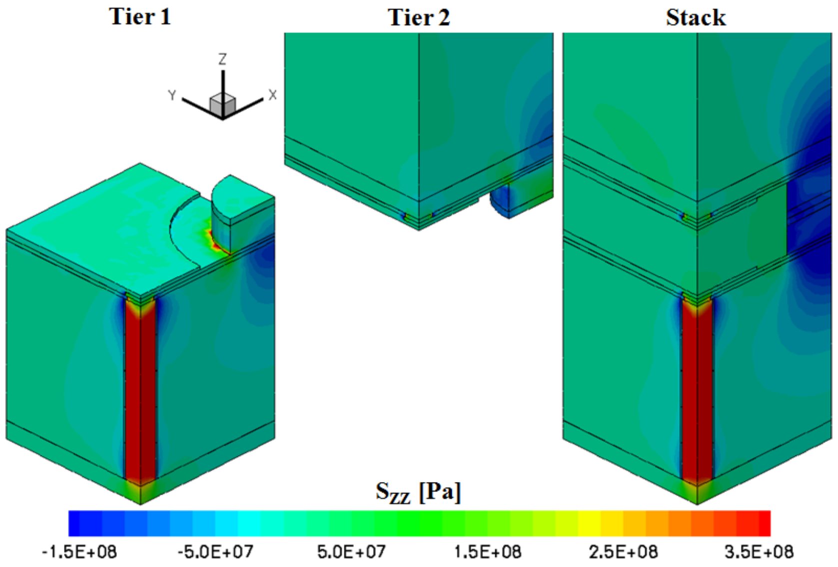

Courtesy of Xiaopeng Xu, Synopsys Inc.

Introduction

Dielectric constant below 2.0 and sufficient mechanical integrity:
-> ULK materials are tailored at multiple scales.

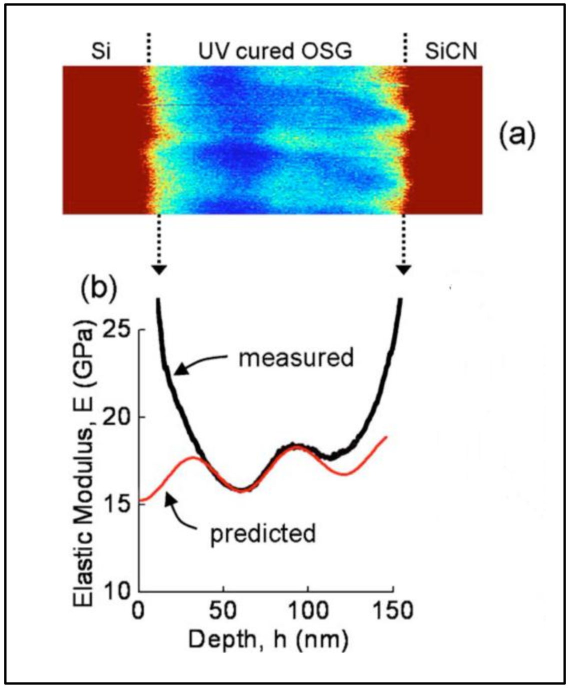

Scale: 100nm

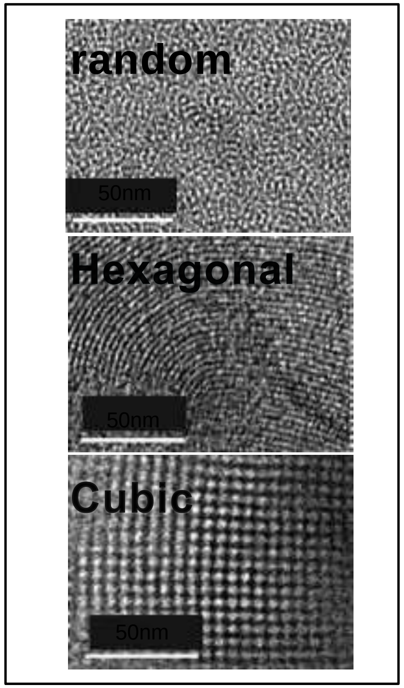

10nm

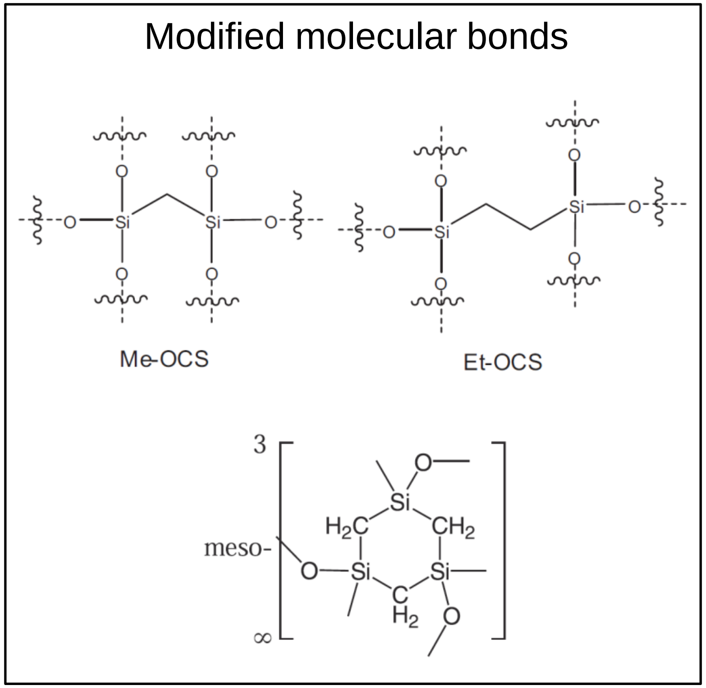

Modified molecular bonds

Molecular and atomic

Characterization of the multiscale properties – structure relationship

Kim et al. APL, Fan et al. Nat.Mater., Dubois et al. Adv.Mater., Landskorn et al. Science

Indenting at Micro/Nano-scale

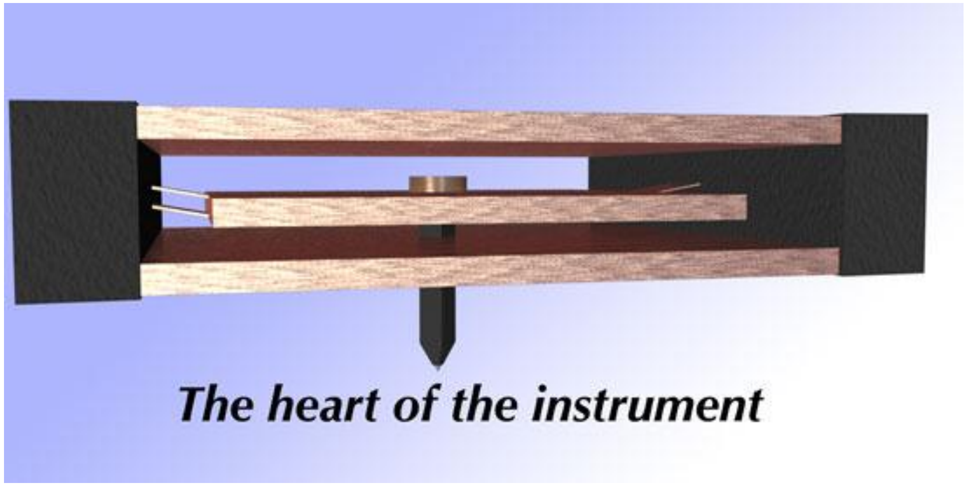

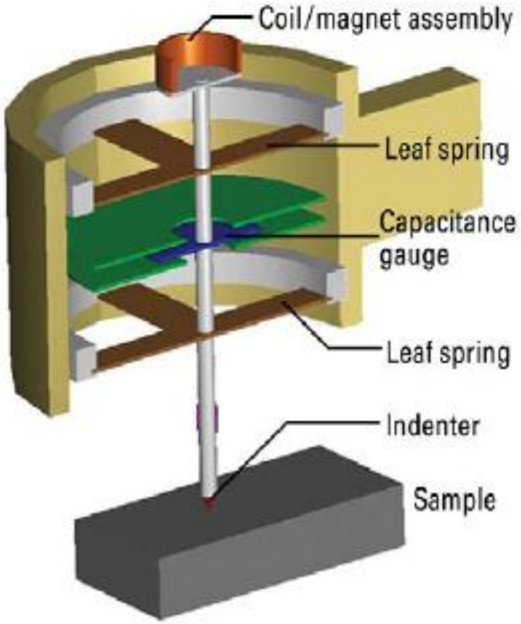

- The heart of a Nanoindentation system lies in the actuator and sensors mechanism
- Capacitive or Electrostatic Force Actuation and Depth Sensing
- Best machine performance: FORCE ~30nN, DISPLACEMENT ~0.1nm

Courtesy of Hysitron Inc. and Agilent Technologies

High resolution nanomechanical testing

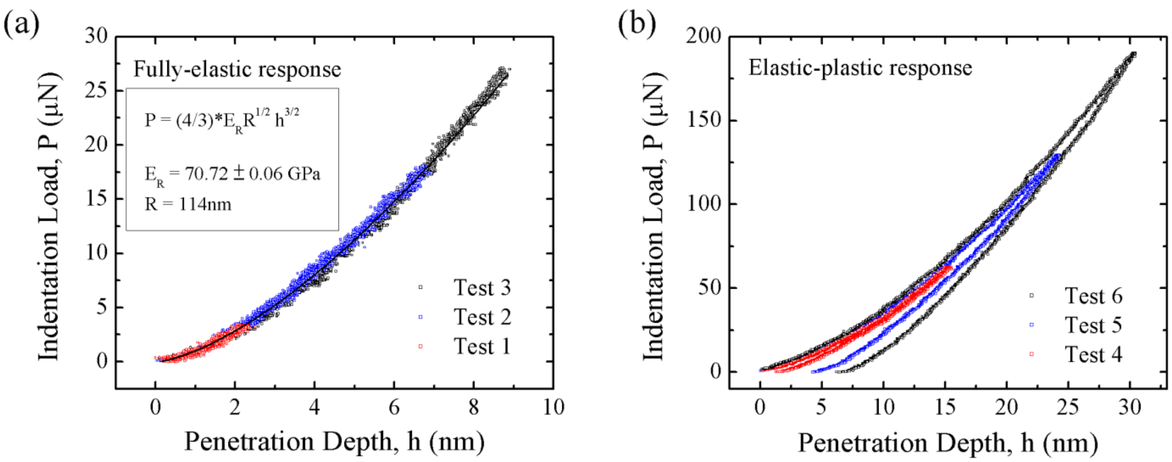

Load-displacement data at single nanometer scale

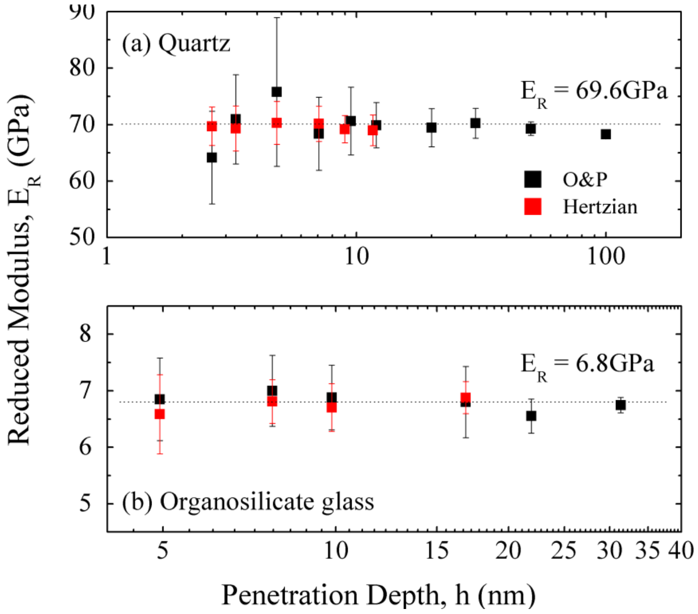

- Displacement length scale similar to the nanostructure of interest
- Nanoscale structure-property relation

High resolution nanomechanical testing

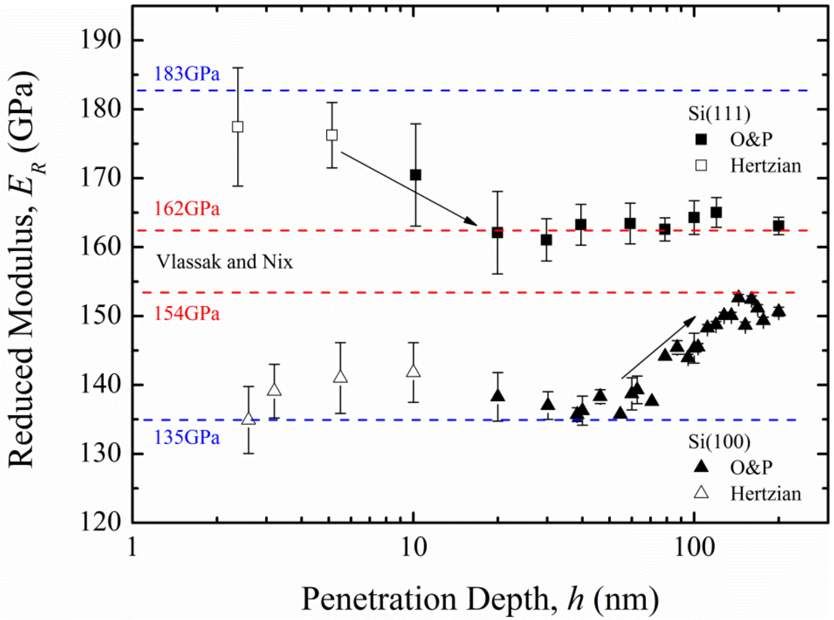

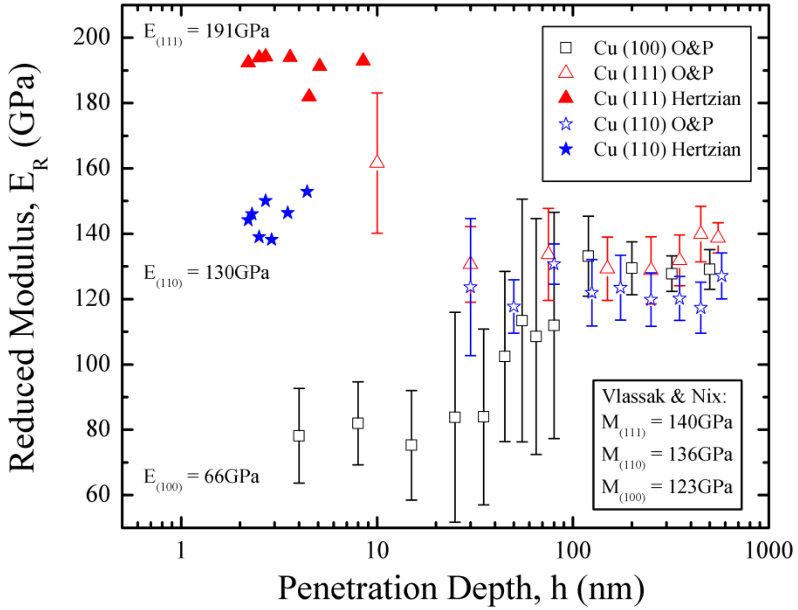

- Small indentation captures more of the structure-related properties
- Large indentation gives average properties
- Elastic-anisotropy is observed if h < 10nm

Self assembly sol-gel template process

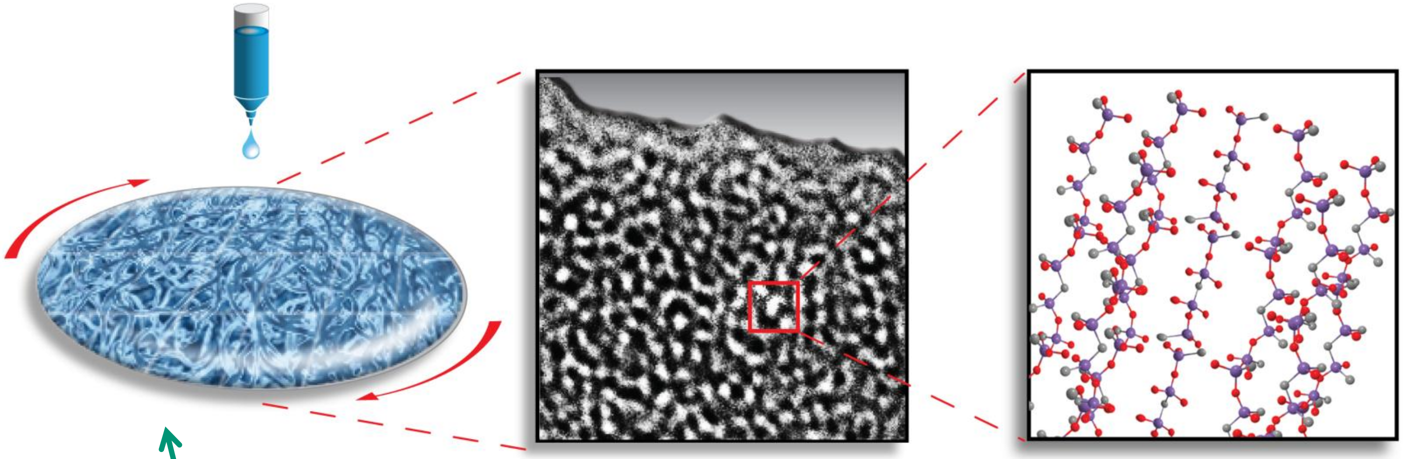

Spin coating + self assembly process

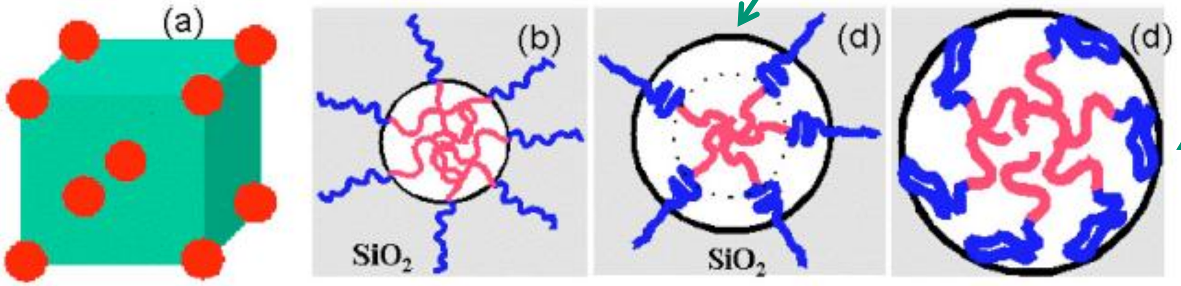

Triblock co-polymer, removed by thermal or UV curing

Evaporation and silanol condensation →

Courtesy: SBA Materials

OSG with different pore topology

Sample description and experimental results for SA-OSG and CVD-OSG films.

Sample	Target *k*	Actual *k*	Porosity, *p* (%)	Thickness (nm)	Elastic Modulus, *E* (GPa)	Cure process
SA-OSG1	1.8	1.80	49	600	3.1 ± 0.1	Thermal
SA-OSG2	2.0	2.08	42	650	3.8 ± 0.2	Thermal
SA-OSG3	2.2	2.21	30	716	5.5 ± 0.3	Thermal
SA-OSG4	2.2	2.25	31	620	6.5 ± 0.3	Thermal
SA-OSG5	2.4	2.37	27	627	6.9 ±0.4	Thermal
SA-OSG6	2.4	2.41	24	693	7.3 ± 0.3	Thermal
CVD-OSG1	2.4	N.A.	25	530	3.7 ± 0.3	UV & Thermal
CVD-OSG2	2.7	N.A.	12	660	6.6 ± 0.7	Thermal
CVD-OSG3	3.0	N.A.	0	520	13.0 ± 1.2	Thermal

Self-assembled organosilicate glass (**SA-OSG**)
Chemical vapor deposited organosilicate glass (**CVD-OSG**)

OSG with different pore topology

Pore arrangement: random vs. ordered domains

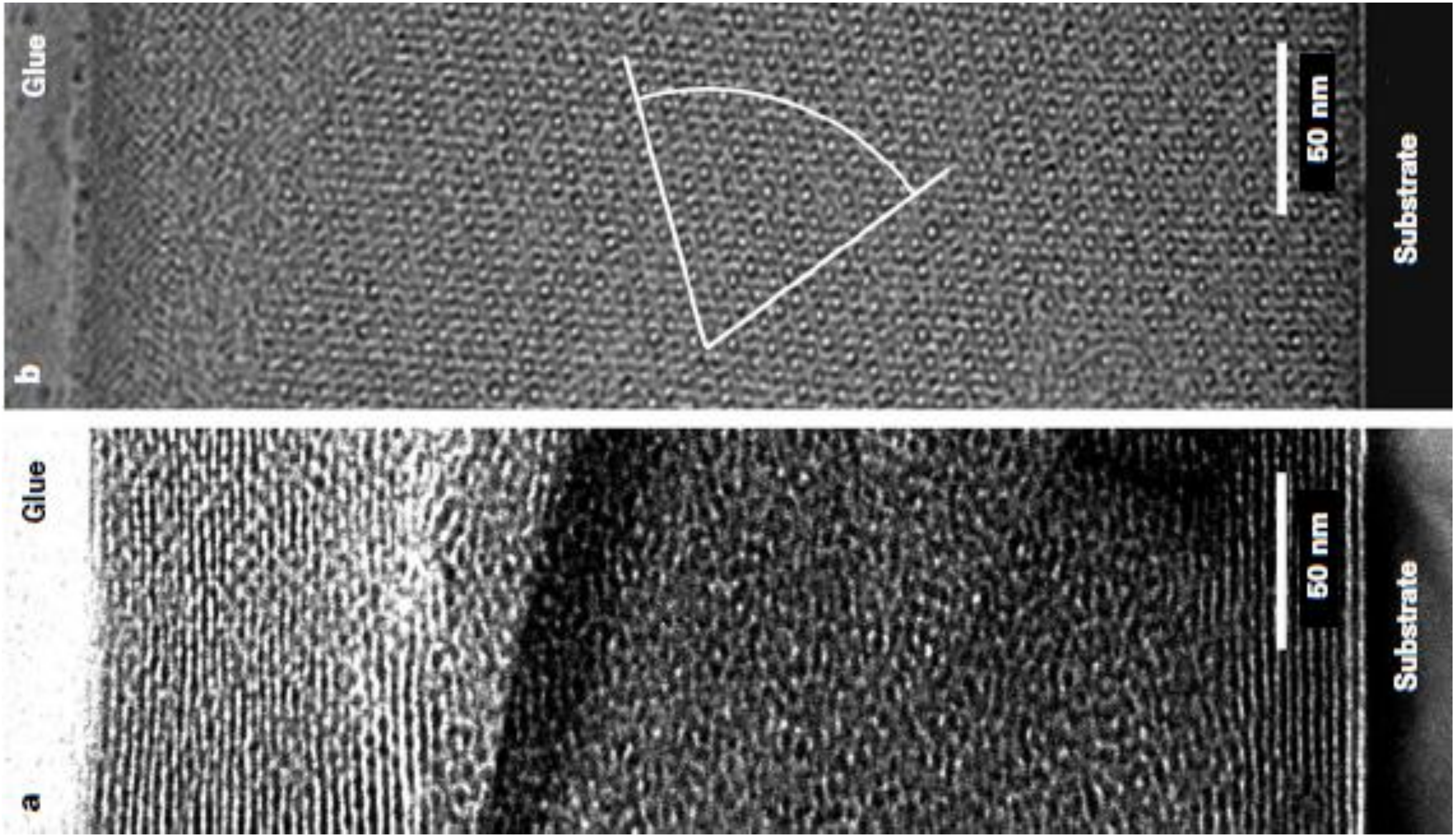

Lu et al. Nature, Maex et al. JAP, Smirnov et al. JJAP

Elastic deformation of CVD-OSG at nanoscale

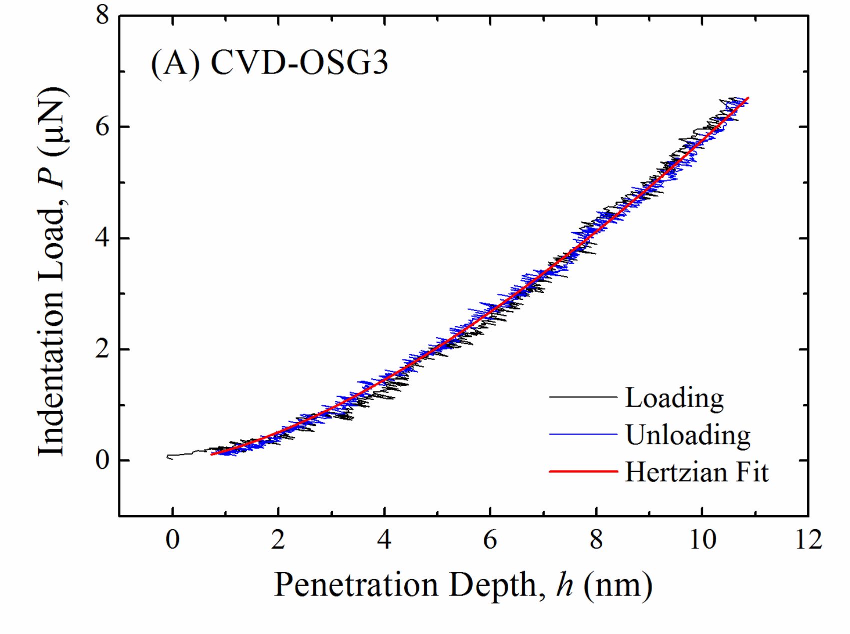

CVD-OSG

- Fully elastic
- Fit well with Hertz model

$$P = \left(\frac{4}{3\pi}\right) E_r R^{0.5} (h - h_0)^{1.5}$$

- Similar to isotropic material
- Consistent for dense or porous CVD-OSG

Elastic deformation of SA-OSG at nanoscale (42% porosity)

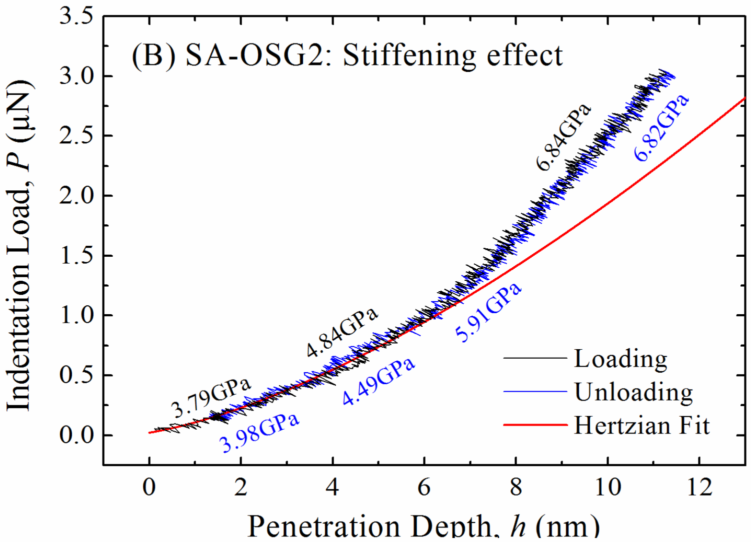

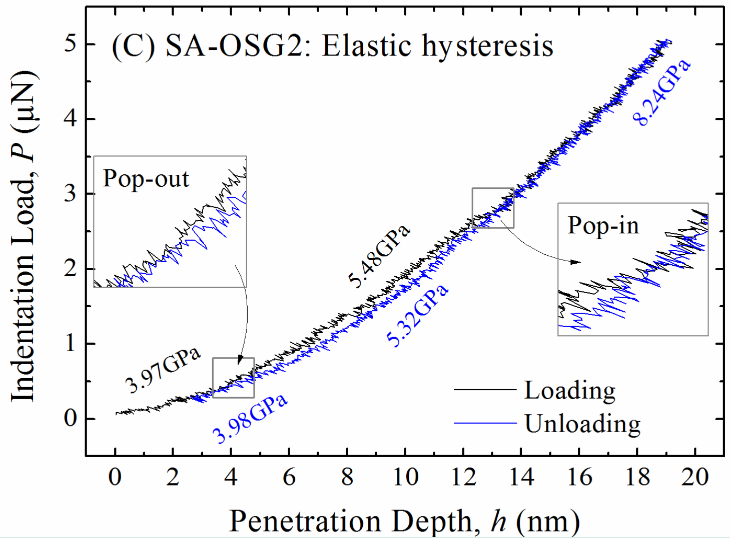

SA-OSG

- Stiffening effect, 4GPa to 7GPa
- Hertz model fits: Initial 3nm of the P-h curve
- 1 out of 4 indentation locations show “elastic hysteresis”
- Pop-in at 13nm of loading curve
- Pop-out at 4nm of unloading curve.
- Match again below 4nm

Elastic deformation of SA-OSG at nanoscale (42% porosity)

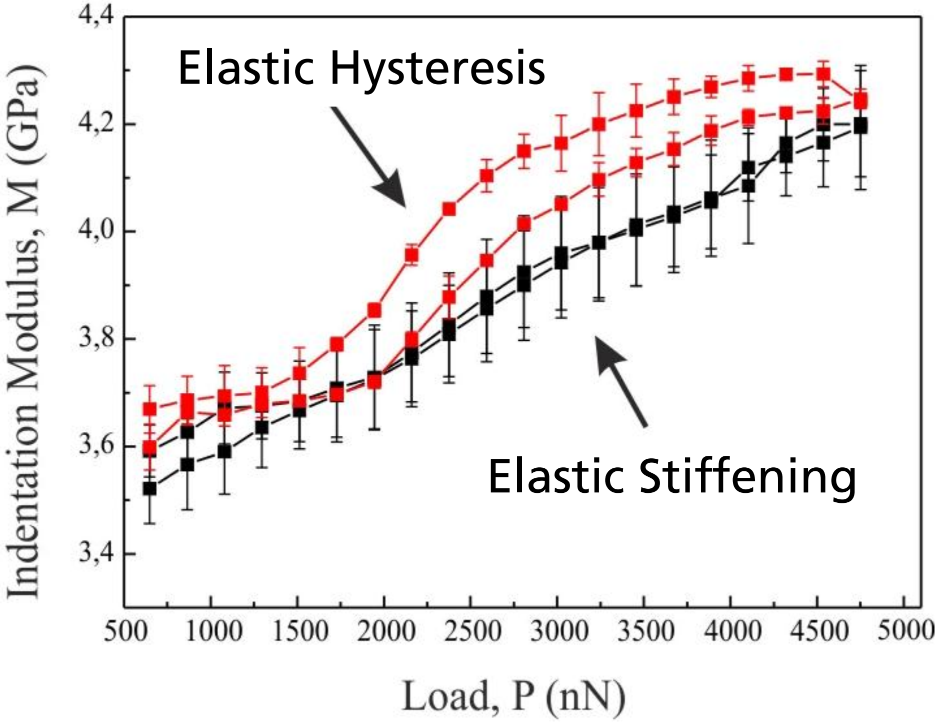

High-frequency dynamic mechanical test:

Atomic-force-acoustic-microscopy **(AFAM)**

Modulus values resolved at P=1µN to 5µN:

- Stiffening effect
- Elastic hysteresis

Deformation mechanism?

- **Elastic stiffening**: pore concentration gradient, topography, or nanocavity strengthening.
- **Hysteresis**: wall-bending or -buckling

Elastic stiffening: Pore concentration gradient

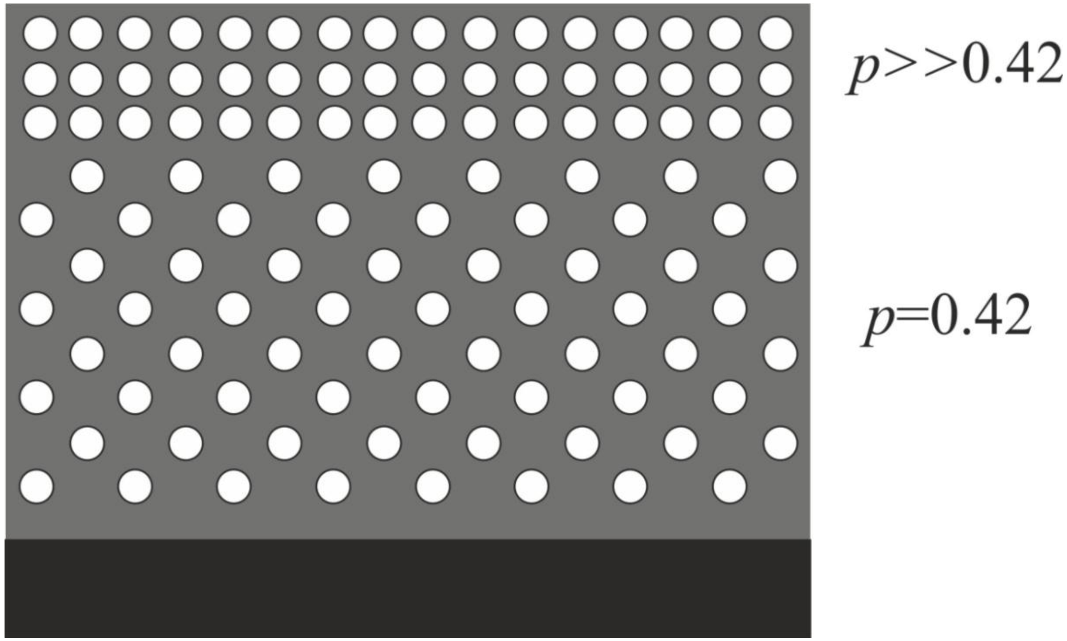

- Pore concentration gradient
- Top layer: porosity>>0.42, thickness<<3nm thick, E<<1GPa
- Bottom layer: porosity=0.42, thickness=500nm, E >10GPa
- Porous structure exceeds the Hashin-Shtrikman upper bound
- Cannot fully account for the observed stiffening effect

Elastic stiffening: Topography effect

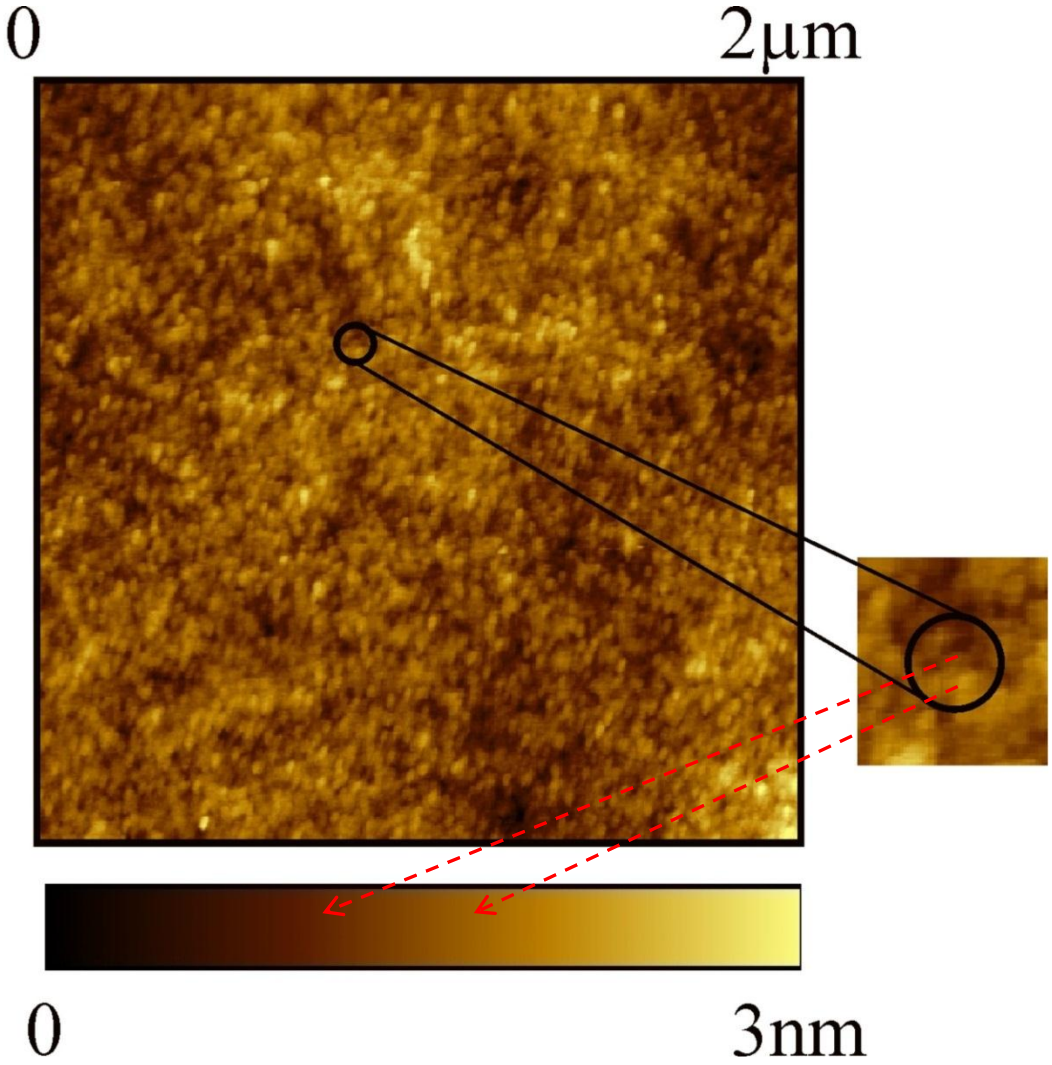

- AFM topographic scan
- No obvious periodicity on the surface
- Indentation contact radius is about 50nm
- Surface roughness within one indentation contact area < 1nm
- **Effect** of topography on indentation data is **small**

Elastic stiffening: Nanocavity strengthening

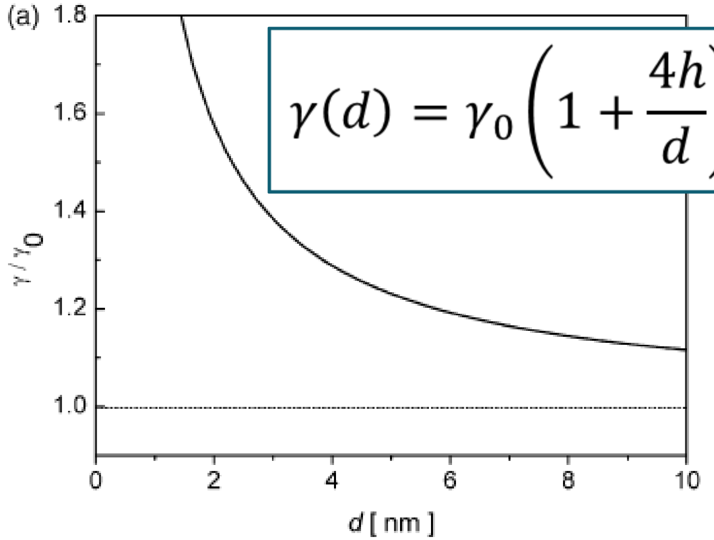

$$\gamma(d) = \gamma_0\left(1 + \frac{4h}{d}\right) + \bar{\alpha}\varepsilon^2$$

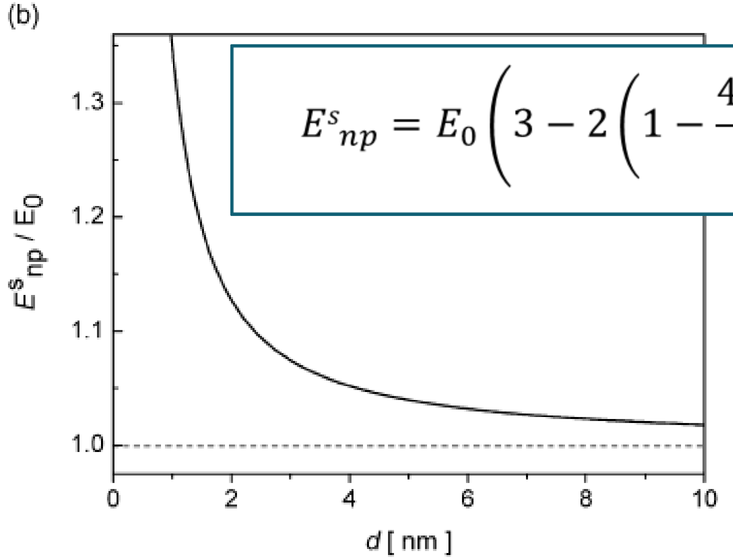

$$E^s{}_{np} = E_0\left(3 - 2\left(1 - \frac{4\gamma(d)}{d}\Xi\right)\right)$$

SA-OSG

- Constant pore size, d=2nm
- Elastic stiffening

CVD-OSG

- Broad pore size distribution, 1nm to 10nm
- Constant E

Ouyang et al., Small, Ding et al. JAP.

Hysteresis: Pore wall bending and buckling

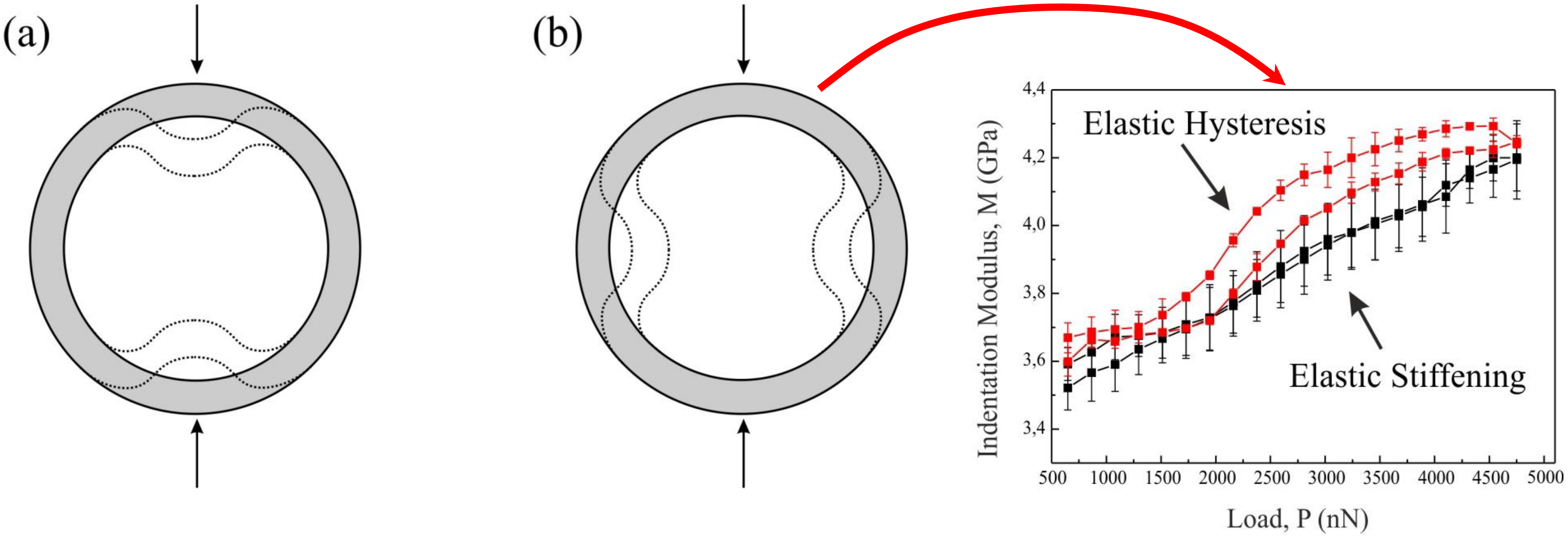

- Under compressive load: bending or buckling dominated deformation
- Buckling of pore walls – structural **instability at critical stress**
- For ordered porous structures, buckling of pore walls is possible, depending on the structure orientation
- **Elastic hysteresis** may be related to pore **buckling dominated** deformation

Topology effect: elastic modulus vs. porosity model

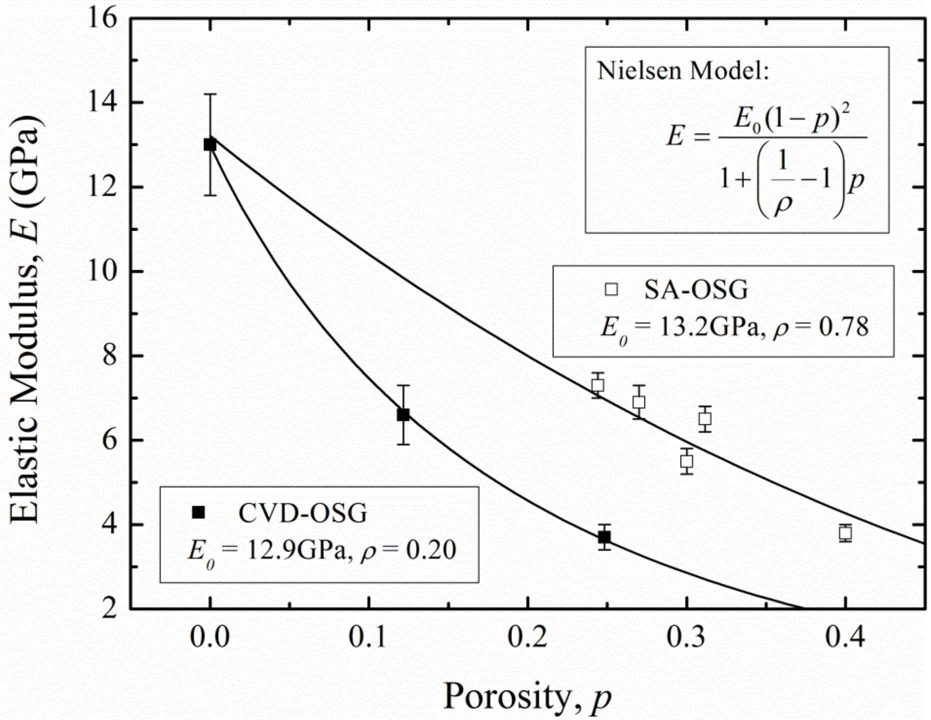

- Mathematical models of E-p relation with one or two variable parameters (n, C for foam model and ρ for Nielsen model)
- The variable parameters are indirectly correlated with the porous structure
- Assuming consistent porous structure

ρ = 0 - 0.4 – shell like pores
ρ = 0.3 - 0.7 – dendrites, ribbons
ρ = 0.6 - 1.0 – closed pores

PAS-positron annihilation spectroscopy

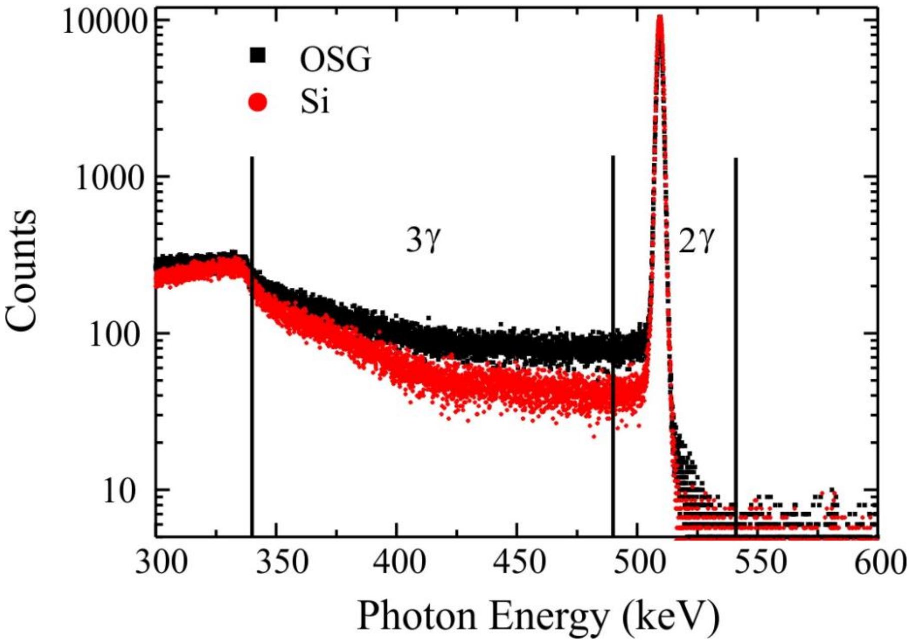

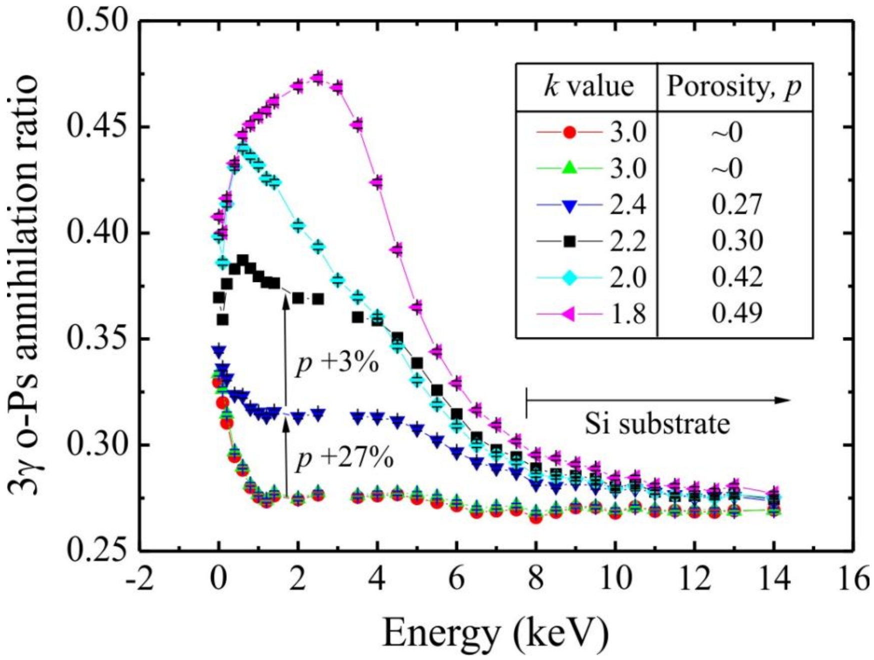

- 3*γ* o-Ps annihilation ratio is proportional to porosity and pore interconnectivity.
- A steep increase of the 3*γ* ratio, when p is increased only by 3% is a clear indication of pore interconnectivity threshold at *p*=0.3.

Courtesy of Marco Jungmann, Uni.Halle

FE simulation of pore topology effect

Random overlapping spherical **solids**

Random overlapping spherical **pores**

Ordered non-overlapping

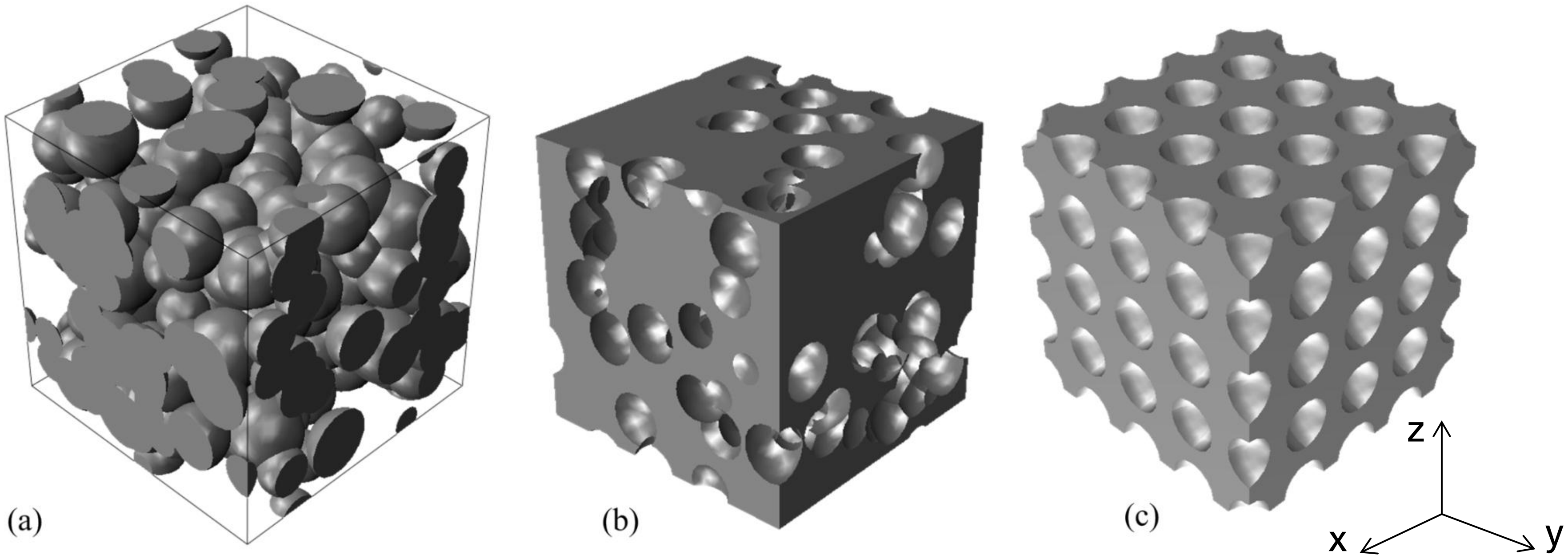

- Homogeneous normal displacement on XY planes, Dz
- Traction-free boundary condition on XZ and YZ planes
- Average stress divided by average strain
- Theoretical threshold value in the FE model is 0.52

A general map of E/Es vs. p for different porous structure

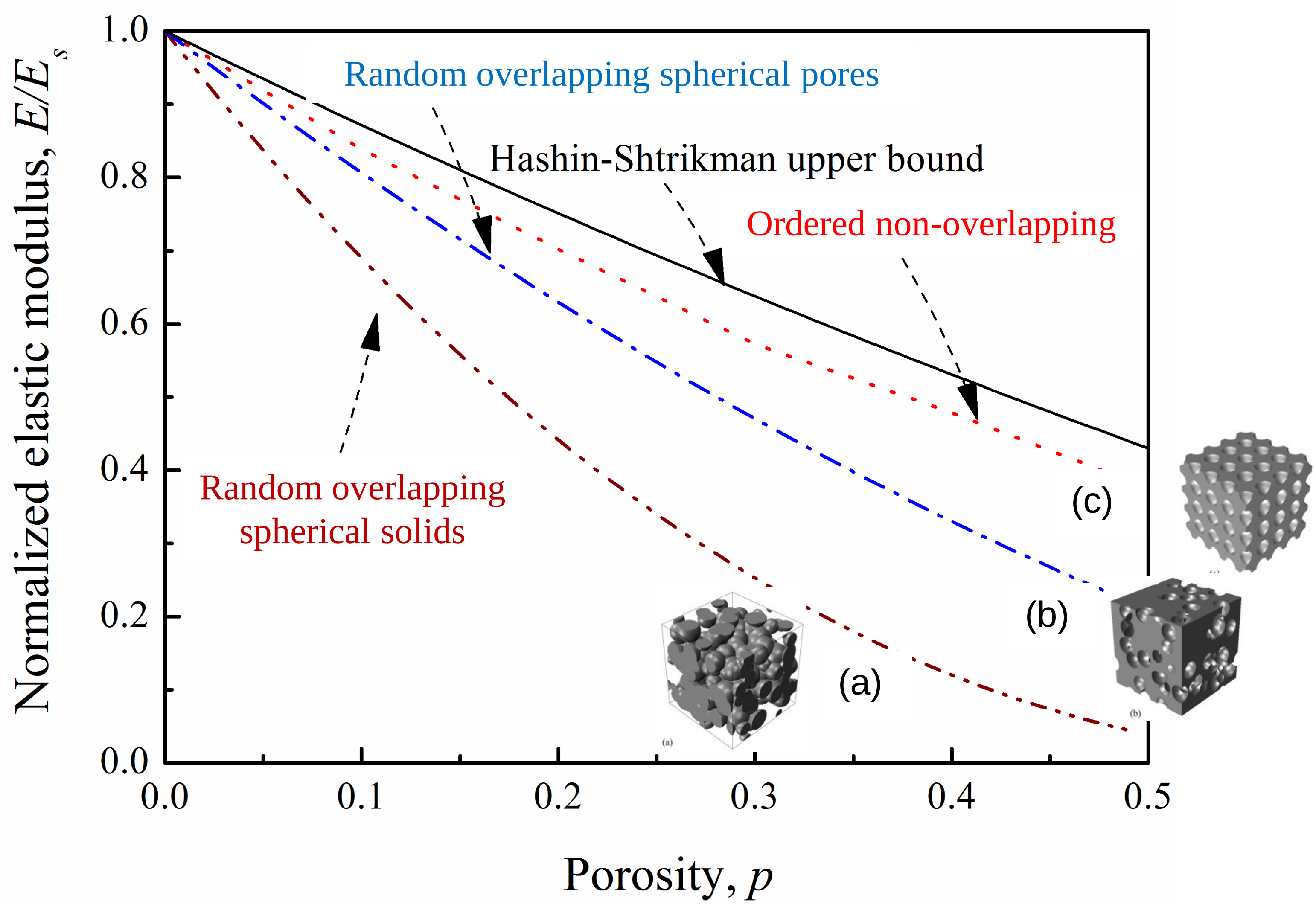

Pore topology prediction

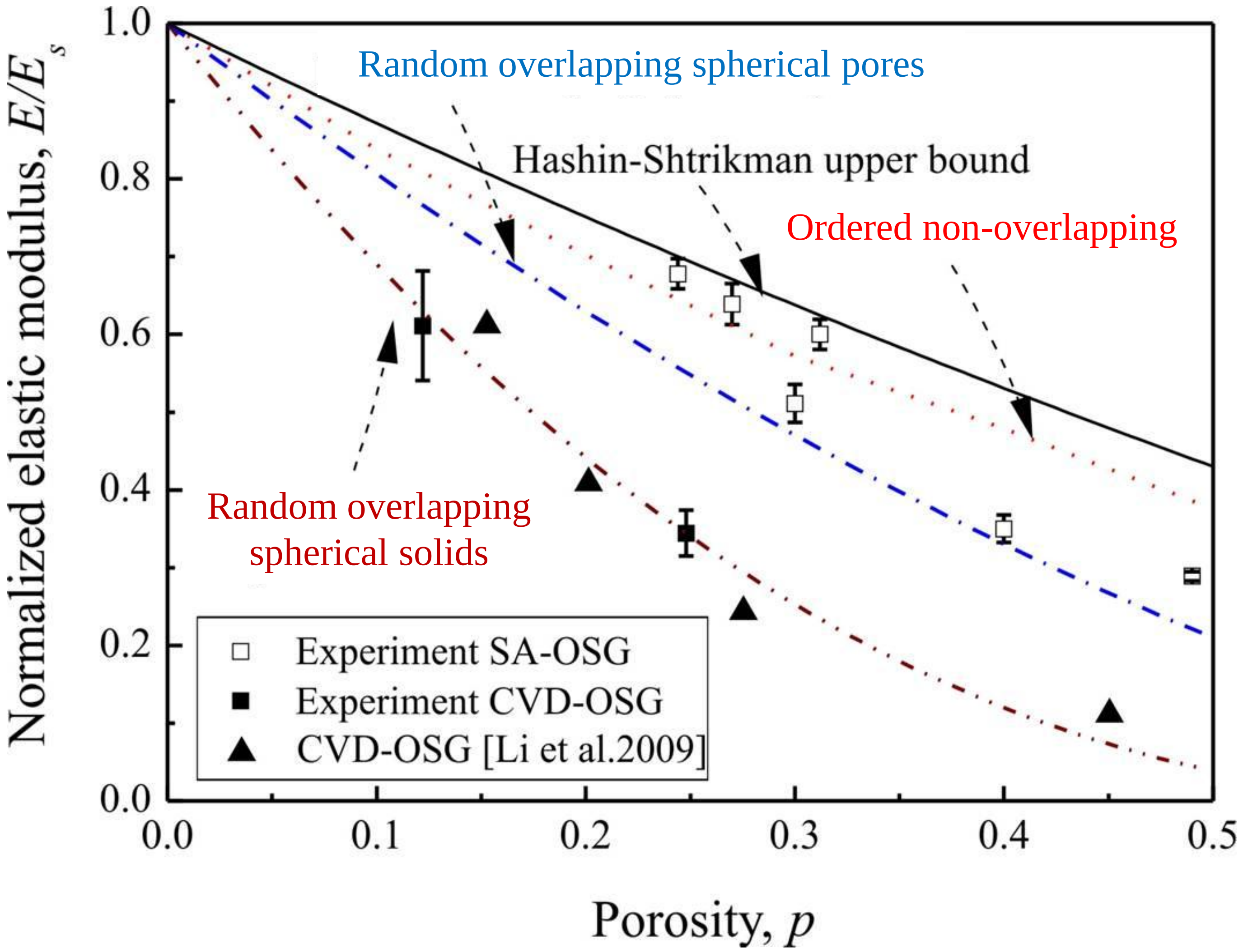

Threshold porosity

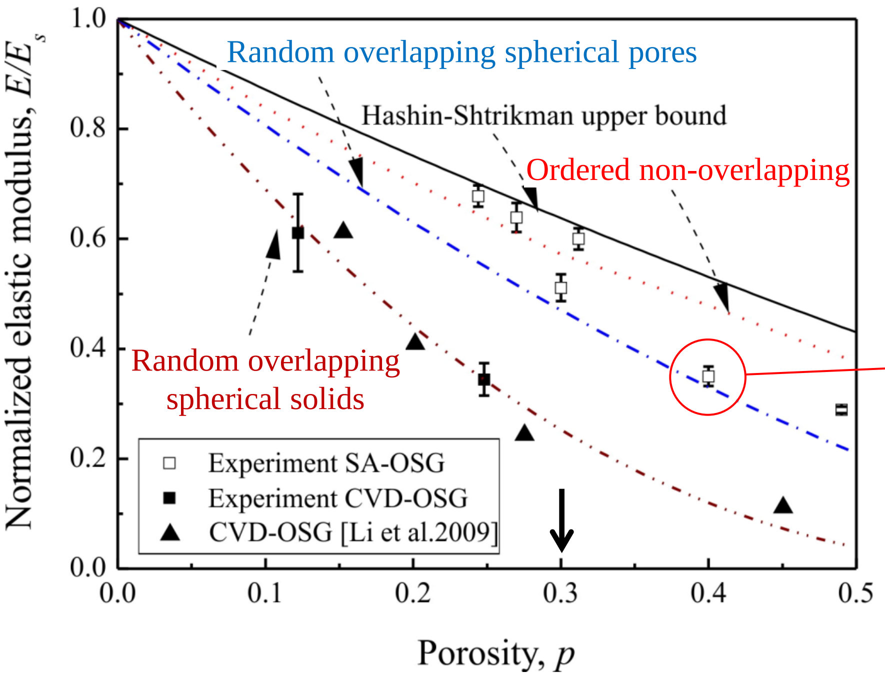

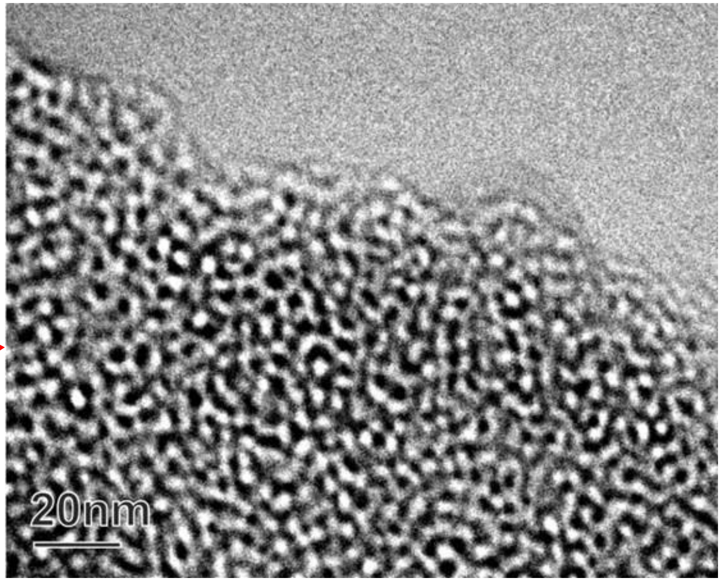

- Threshold value before pores begin overlapping, $p_{threshold}=0.3$ for the SA-OSG.
- TEM image at p=0.42 shows random overlapping spherical pores with very narrow pore size distribution.

Coefficient of Thermal Expansion

CTE

Motivation for effective CTE measurement

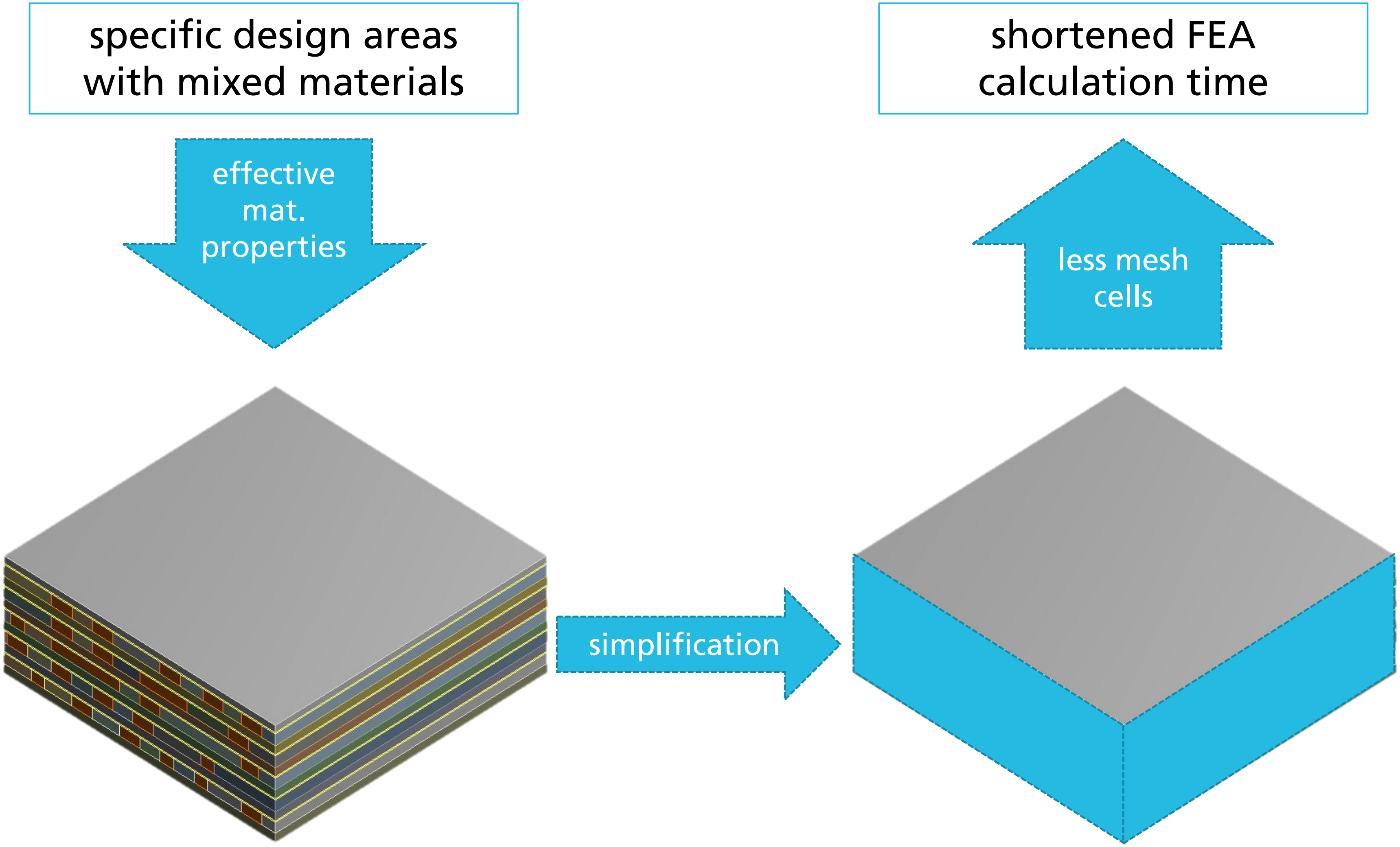

specific design areas with mixed materials

effective mat. properties

simplification

shortened FEA calculation time

less mesh cells

CTE – Volumetric balance

FIB cut lines in red

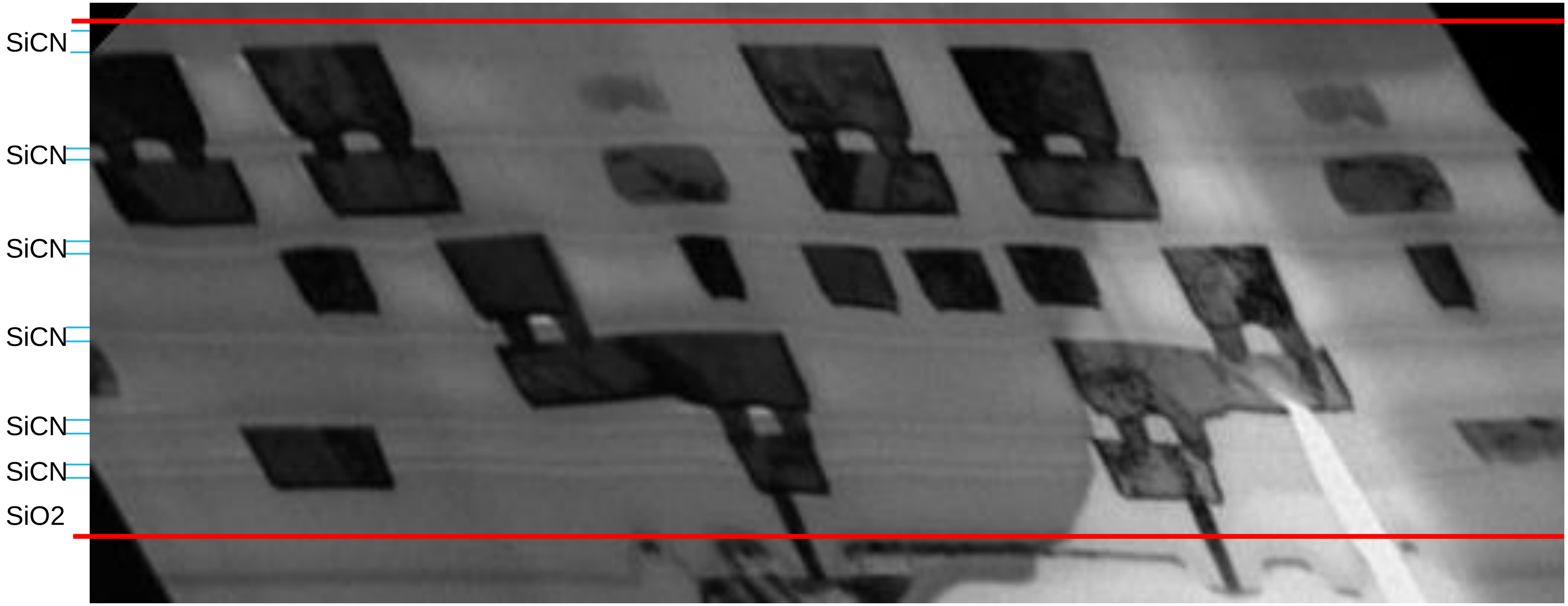

Note: We are measuring an effective CTE value, including some of the SiO_2 at the bottom CA layer, as well as SiCN layers in between.

CTE measurements of BEoL: Preparation

First approach to determine CTE for Cu/ULK for a partially deprocessed 3DIC, by combination of FIB cutting and SEM (heating stage holder).

- ☐ isolate a bar
- ☐ separate in two bars of same length
- ☐ mount on heating stage and measure the gap in the middle during the experiment

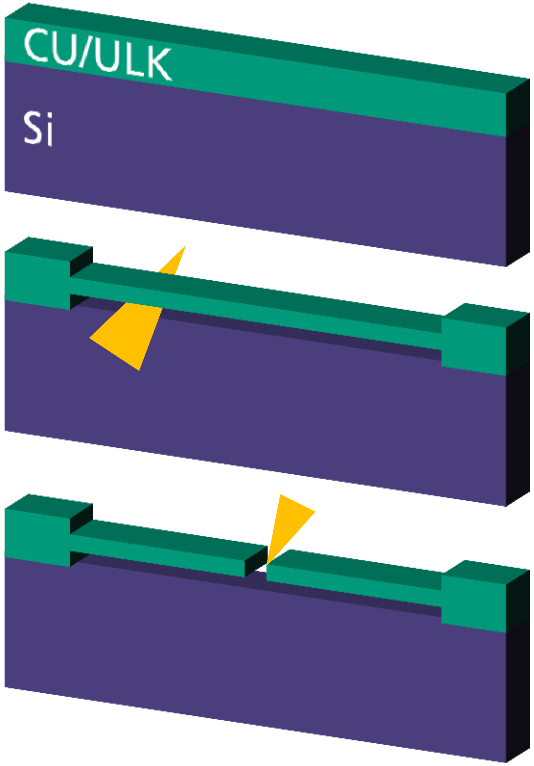

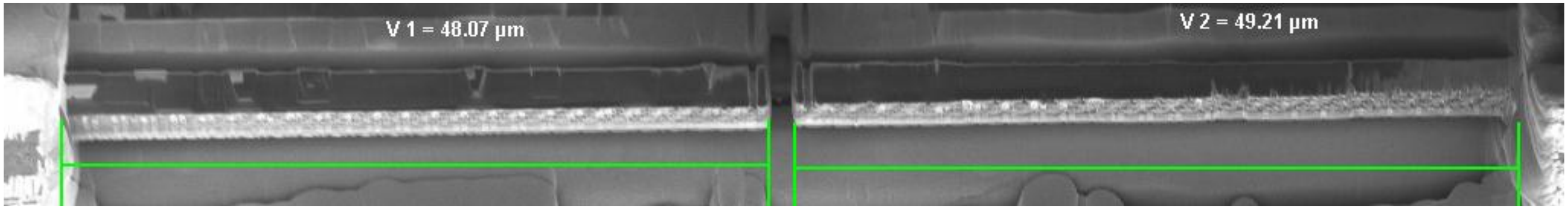

CTE measurements of BEoL: Stack

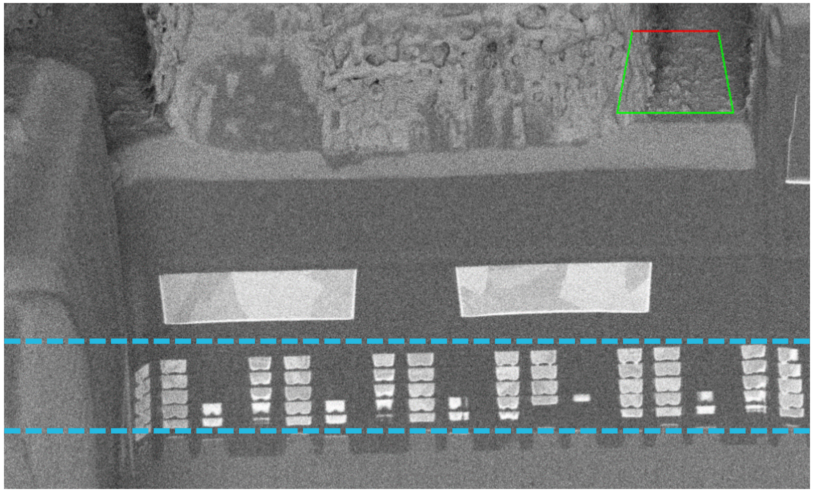

Full metallization stack

TEOS/SiN Passivation and Al

V5-M6 Thick Cu/(F)TEOS

M1-M5 Cu/ULK

FIB cutting to form two freestanding 50µm »cantilevers« which are free to expand towards the center (only Cu/ULK)

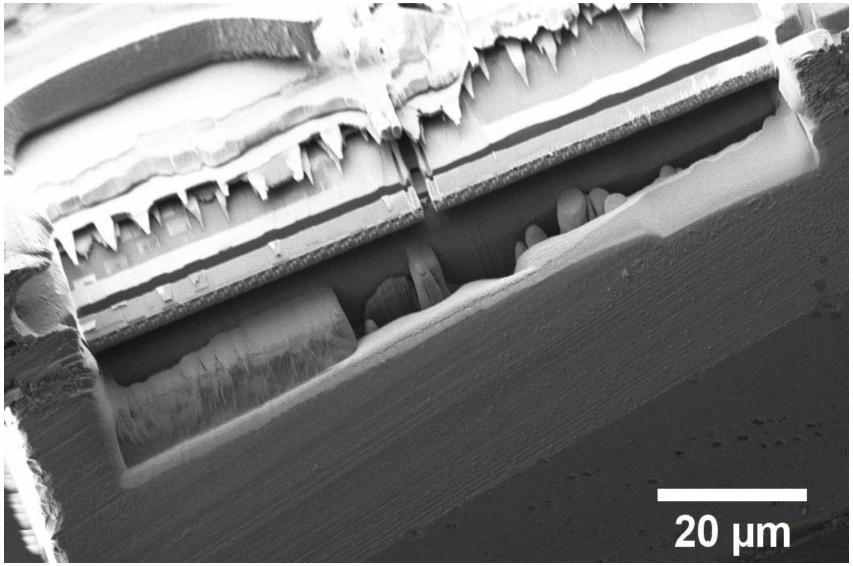

CTE measurements of BEoL: Basics (2)

$$\alpha_l = \frac{\Delta l}{l_0 \cdot \Delta T}$$

$$\Delta l = \Delta gap + \Delta Si$$

$$\Delta gap = gap_{25°} - gap_{250°}$$

$$\Delta Si = Si_{25°} - Si_{250°}$$

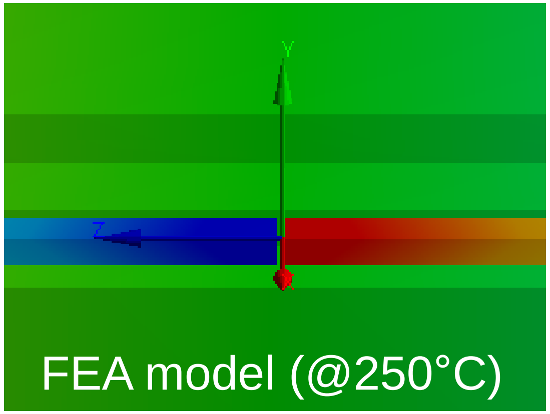

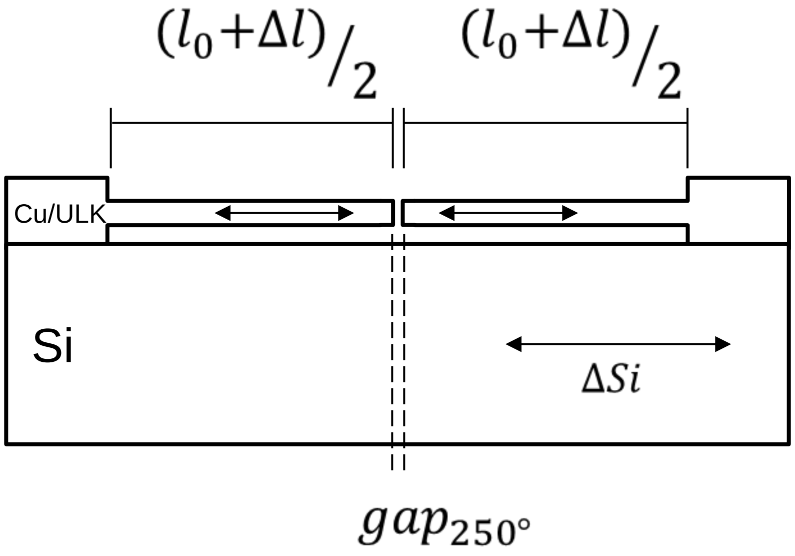

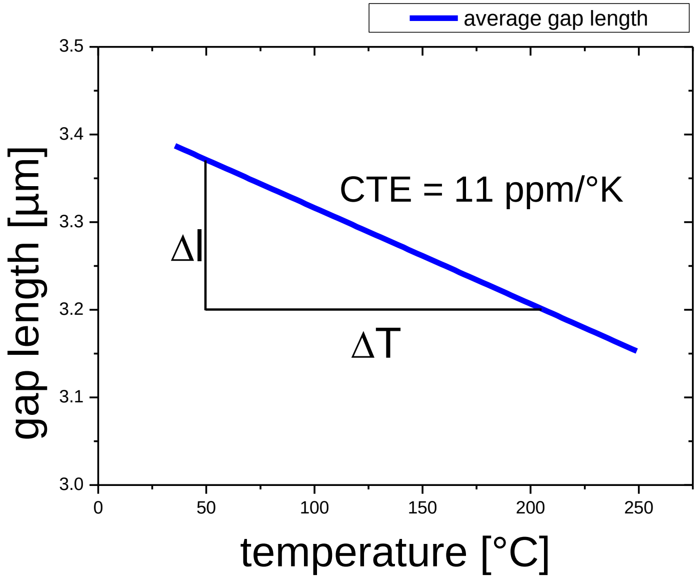

Effective CTE M1-M5/ULK

spot	1x	2x	3x	4x	4y	5	6
CTE (ppm/K)	6.7	6.1	5.9	5.6	8.0	7.1	11
Cu %	17.3%	17.0%	18.4%	18.3%	18.3 %	23.8 %	23.8 %

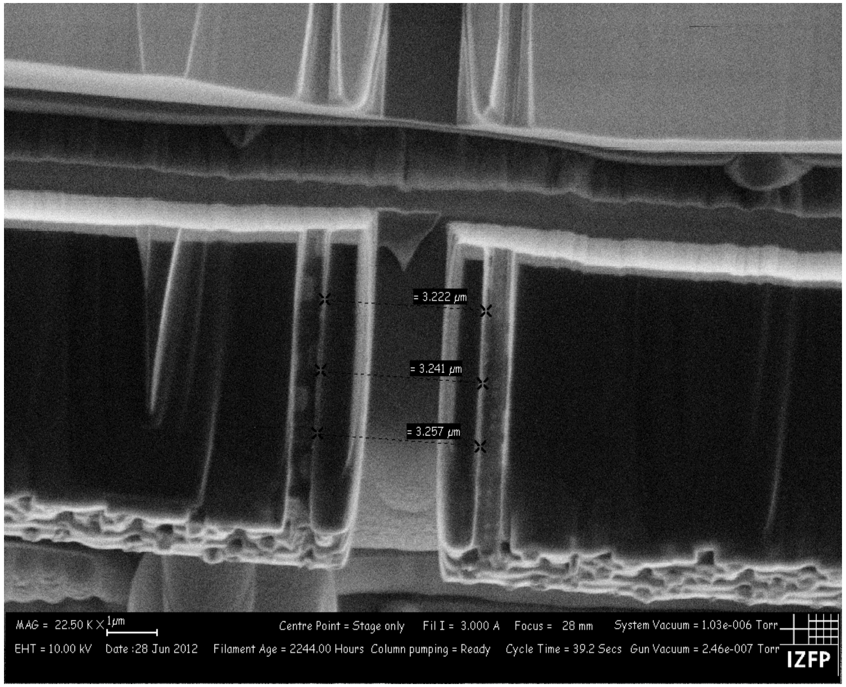

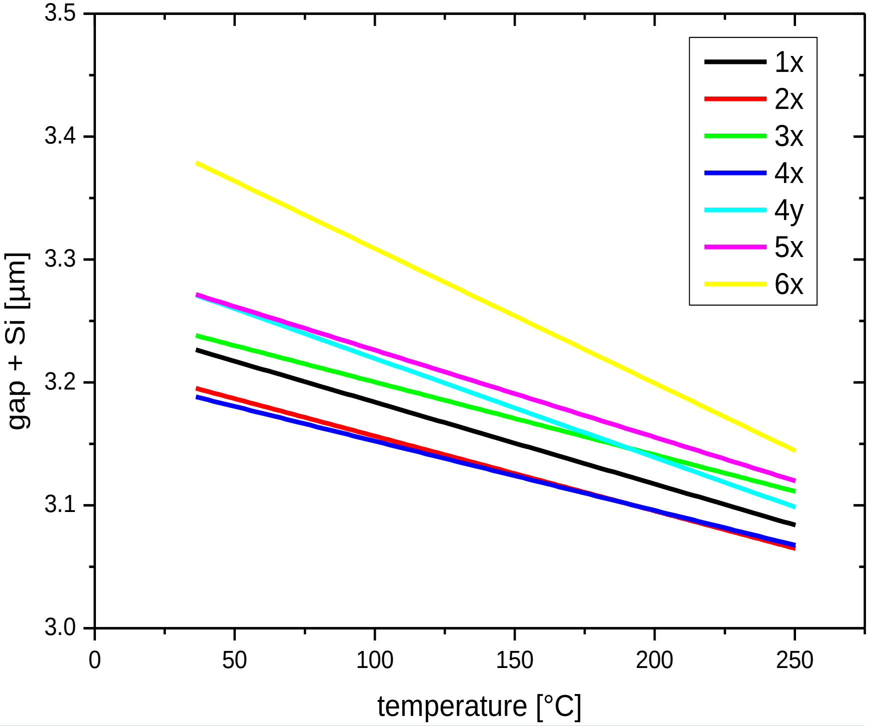

CTE – FEA simulation

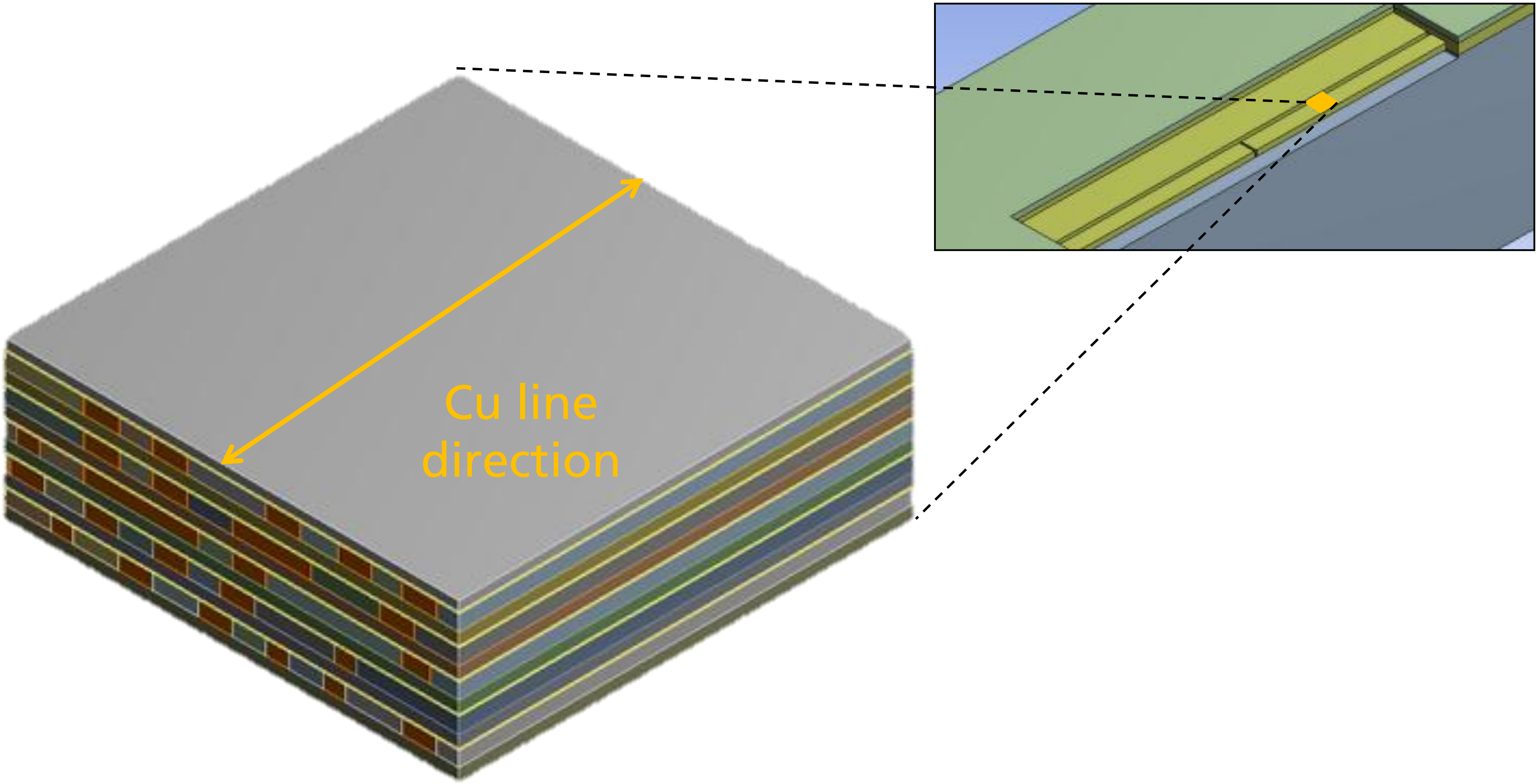

4 x 4 x 1.2 μm^3 part of CTE-bar

CTE – FEA simulation

deformation in z direction – Cu inline

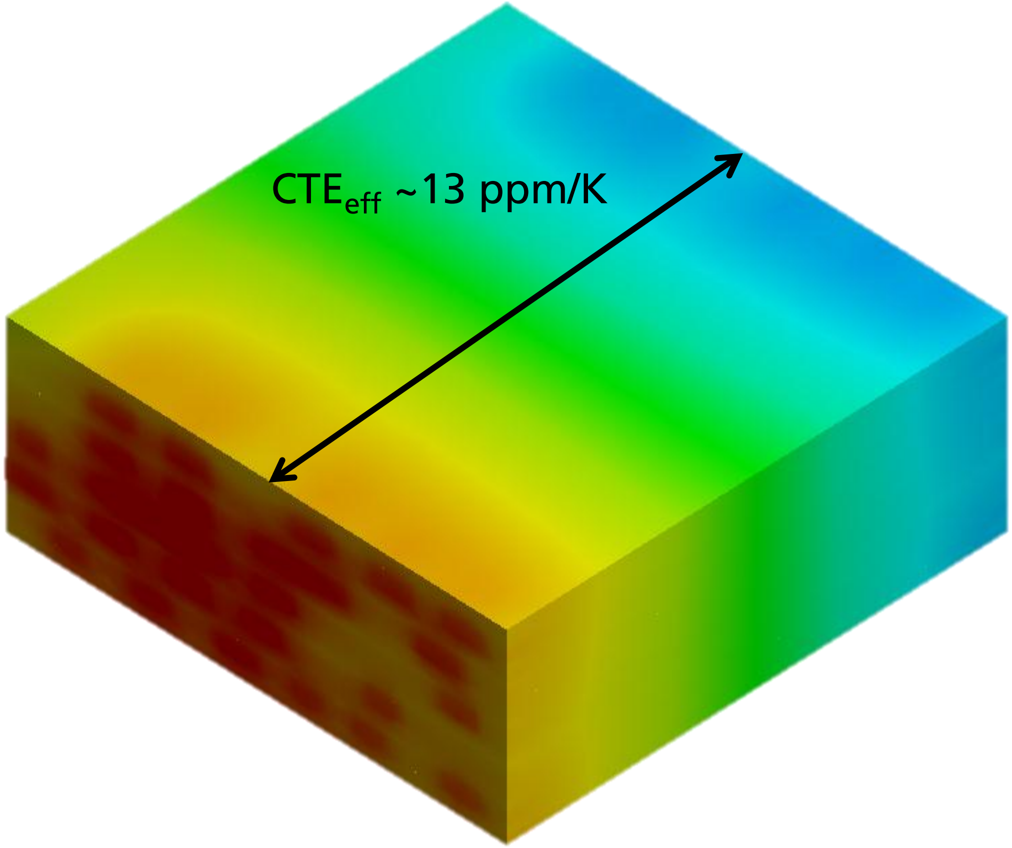

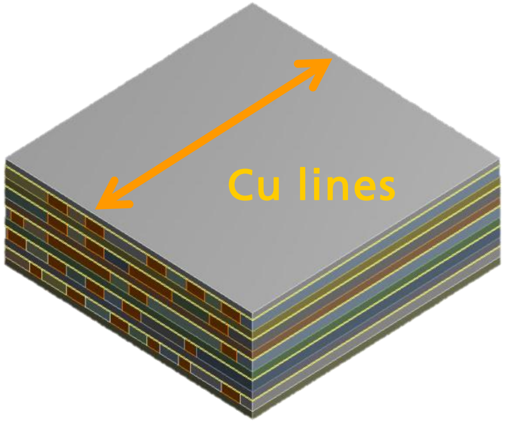

Cu randomly distributed
Cu density from real IC
dim. 4x4µm²

CTE – FEA simulation - Cu line direction

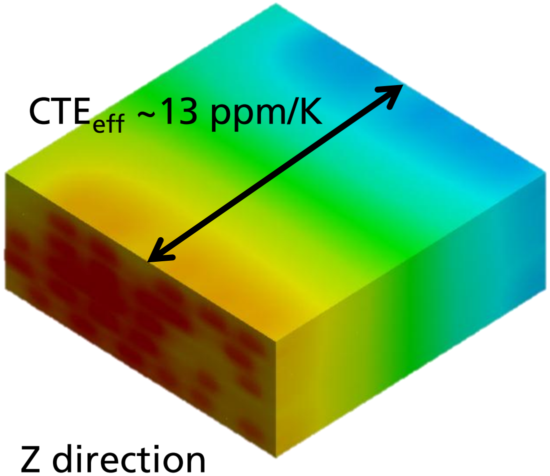

Z direction

FEA results

- effective CTE highly constrained to design
- more information about Cu distribution and orientation needed
- simulated CTE$_{eff}$ ~ 5.5 – 13 ppm/K matches exp. data

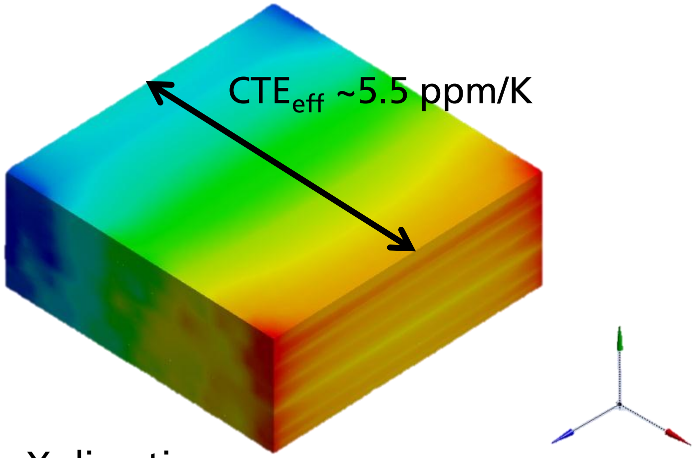

X direction

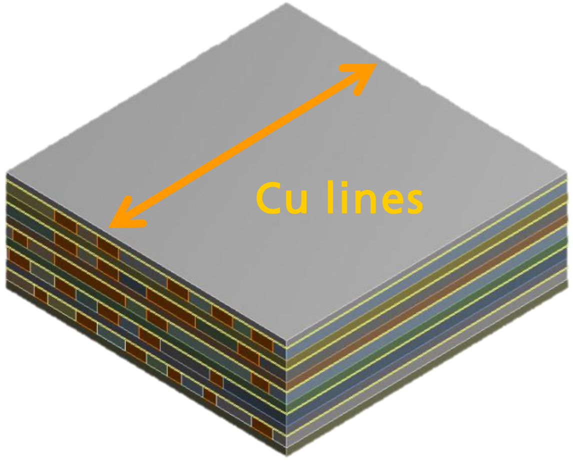

Adhesion

WEDGE-INDENTATION TECHNIQUE

Wedge Indentation Experiments

Hysitron TI-950

Low-k materials

- Porous Spin-on glass (Methyl-silsesquioxane: **MSQ**)
- Densed PECVD glass (Black Diamond: **BD**)

MSQ , JSR LKD5102

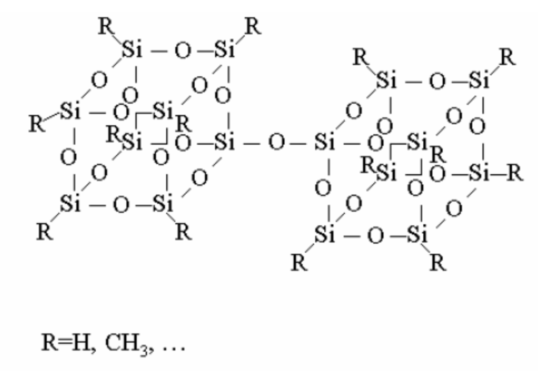

R=H, CH_3, …

BD, Applied Materials

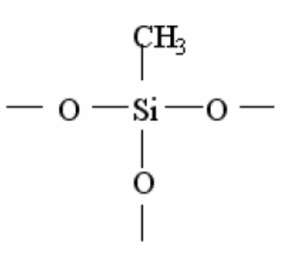

Wedge indentation

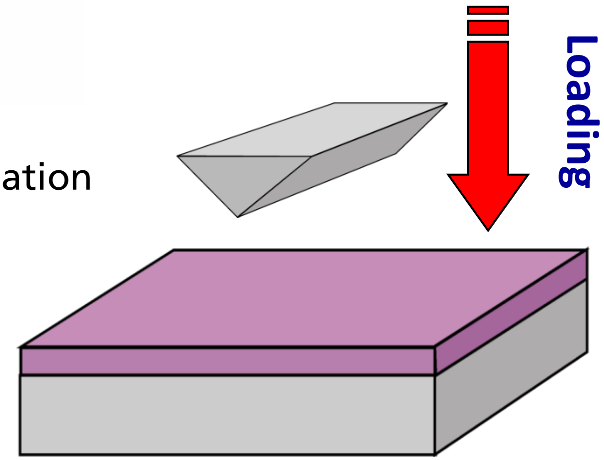

Indentation Induced Interfacial Fracture

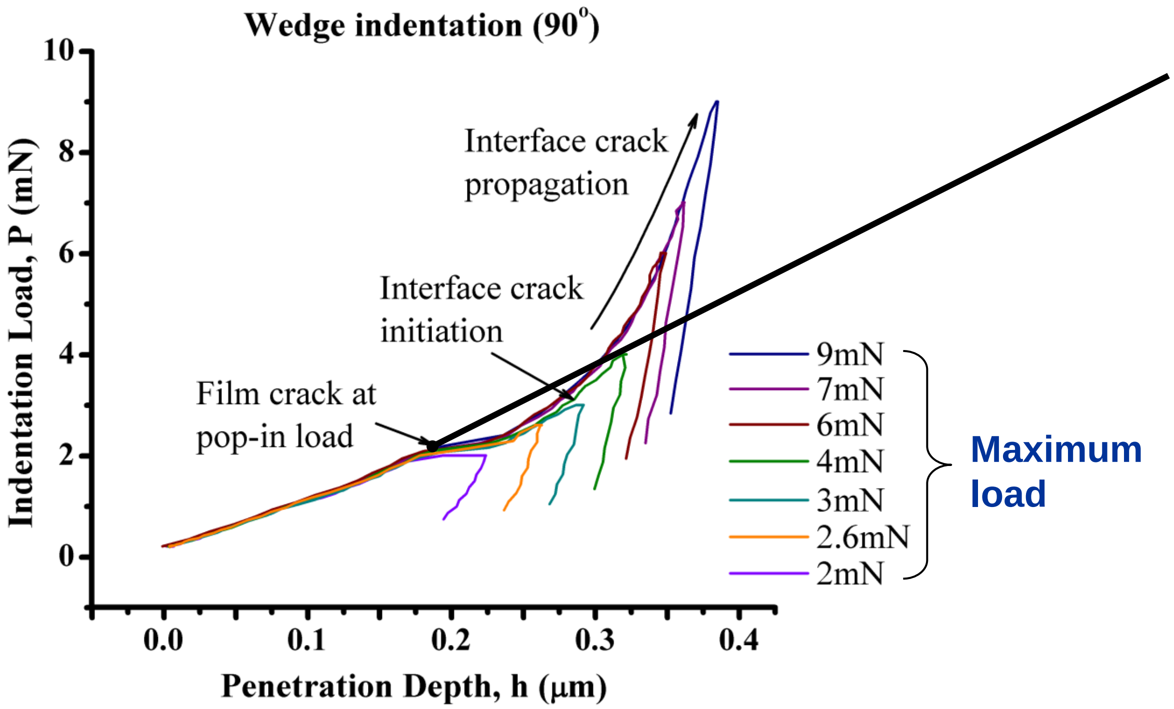

Maximum load

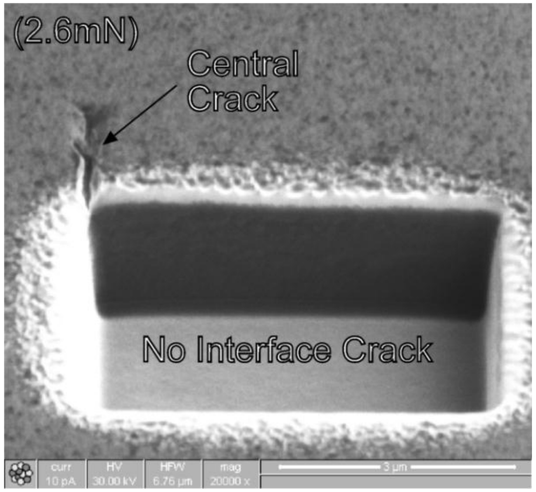

Indentation Induced Interfacial Fracture

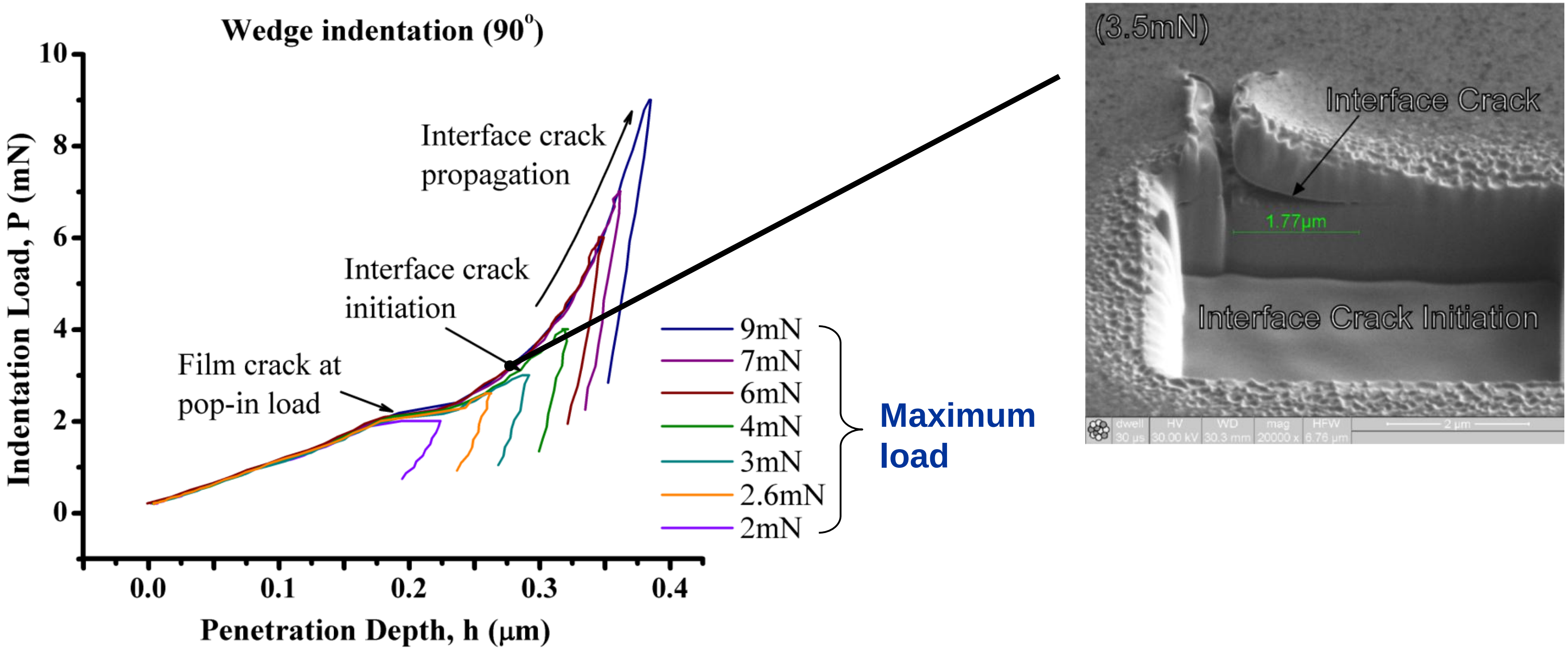

Maximum load

Indentation Induced Interfacial Fracture

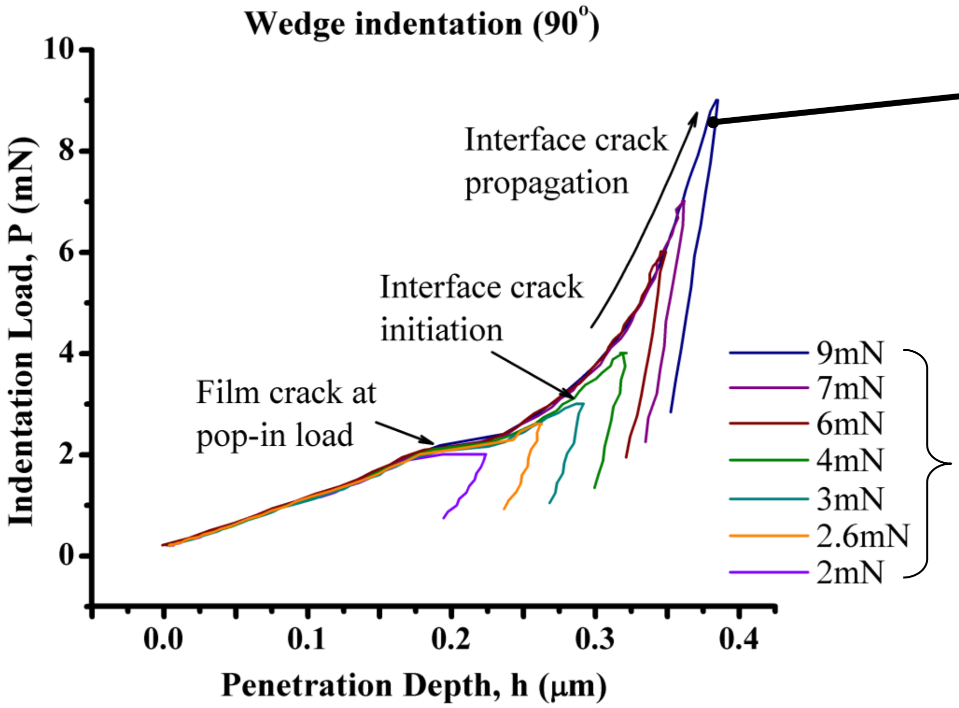

Maximum load

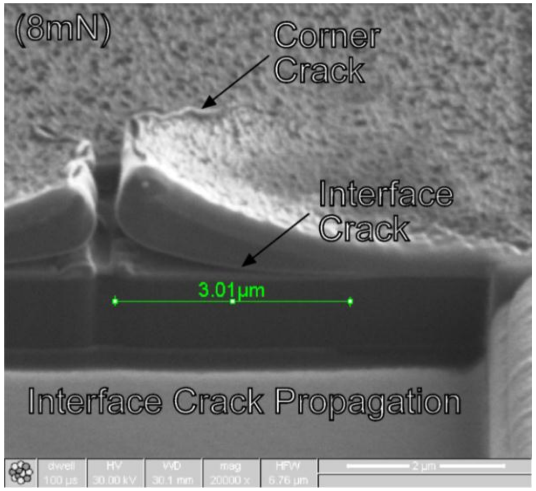

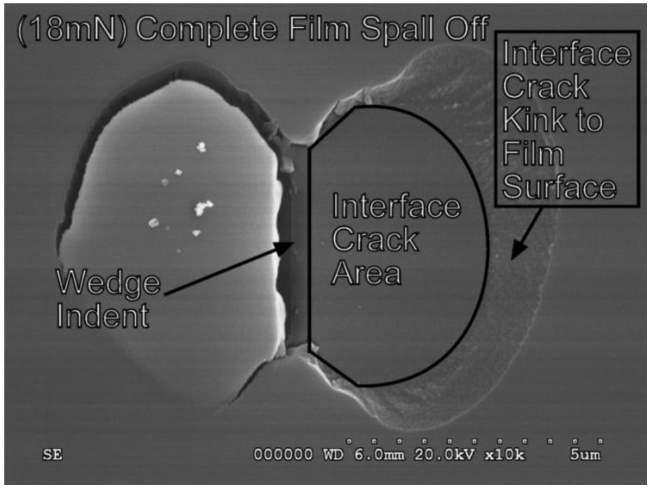

Delamination Shape

Interfacial toughness of varying film thicknesses

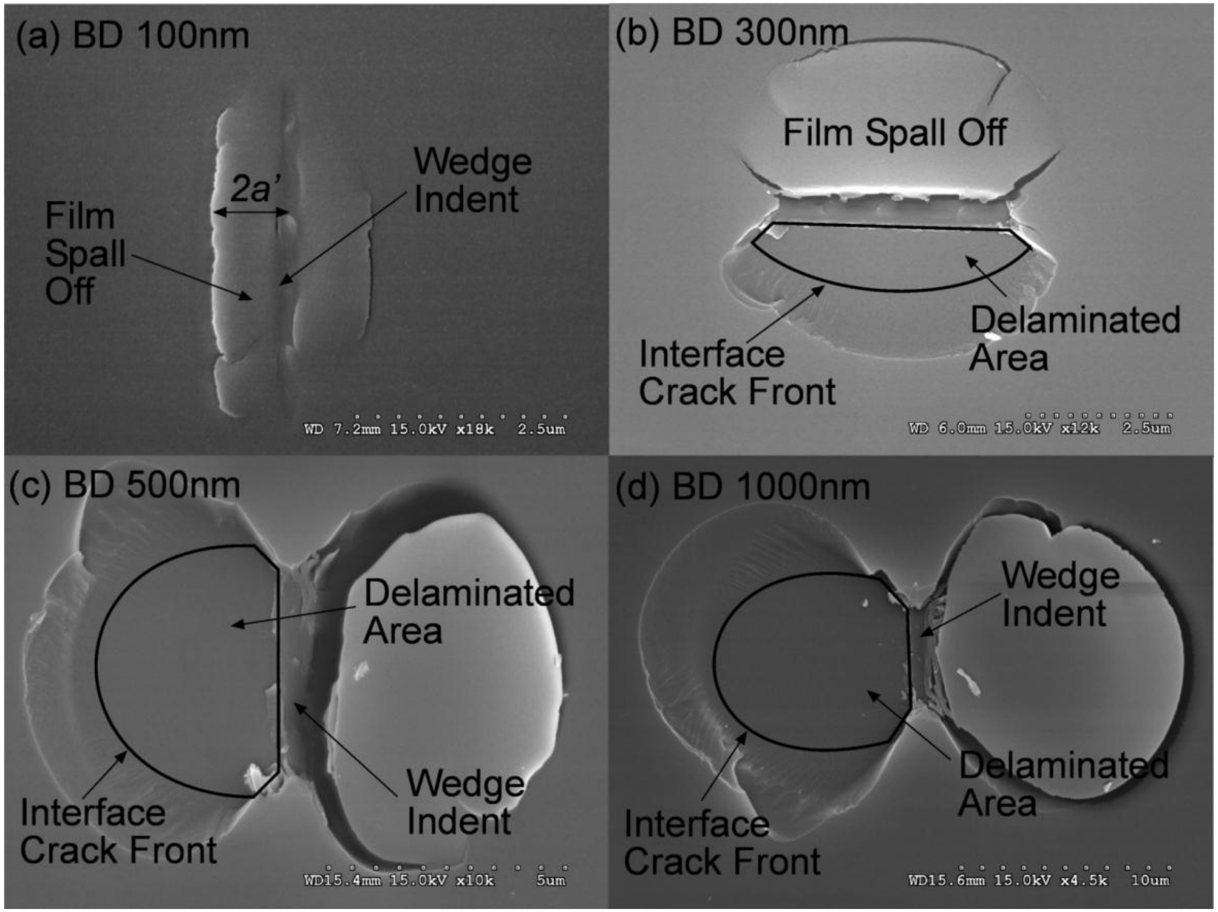

Varying film thickness results in different delamination shape.

Wedge Indentation – automated image analysis

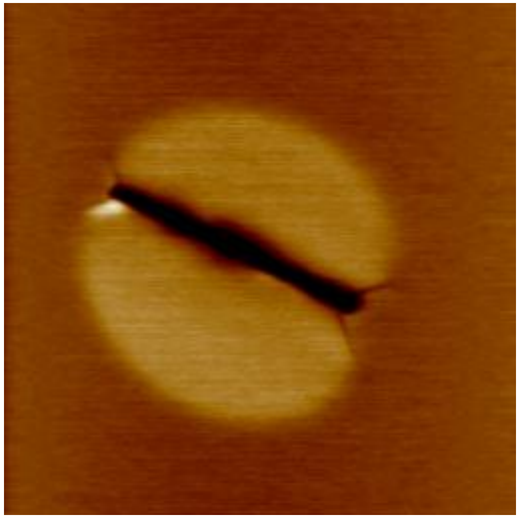
topography map

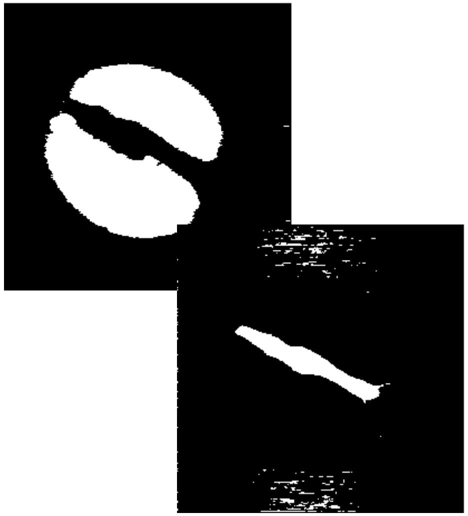
analysis

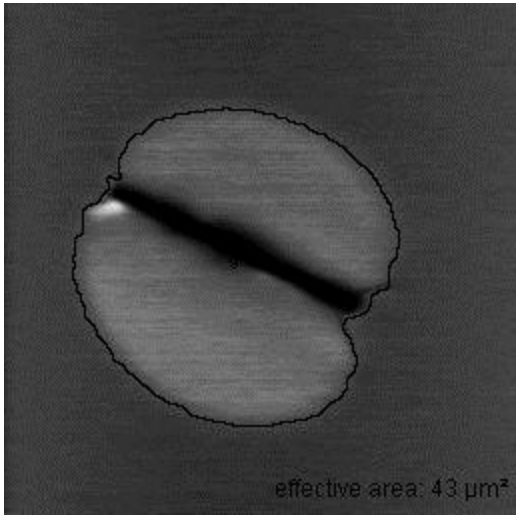

computed area

- Automated indentation and crack area mapping procedure with high local resolution
- Crack area and adhesion calculation software routine.

Wedge Indentation technique

Wedge Indentation results

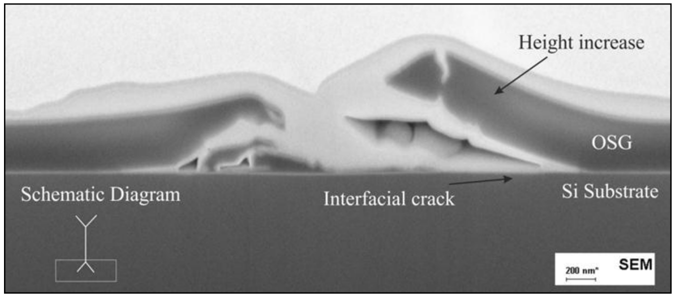

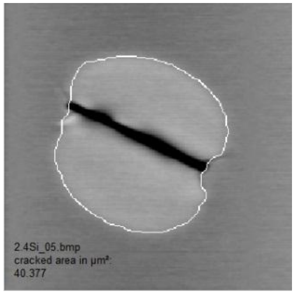

Sample	Gc (J/m2)	error	E (GPa)	error
k = 2.7	4.24	0.29	8.86	0.63
k = 2.5	3.38	0.31	6.22	0.19
k = 2.4	2.79	0.18	4.42	0.32

Advantages:

- No sample preparation, fully automated.
- Statistical variation that represents the true adhesion variation, not the error of the experiment or sample prep.

4 Point Bending results

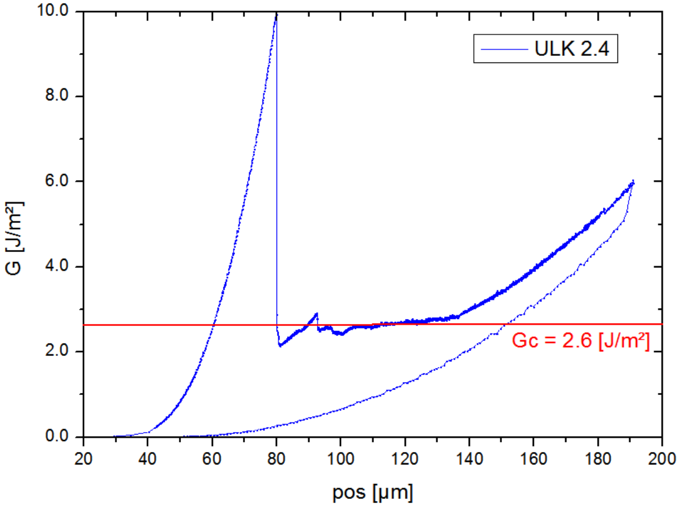

Sample	Gc (J/m2)
k = 2.7	4.3
k = 2.5	-
k = 2.4	2.6

Conclusion

- Mechanical test at a length scale similar to the pore size is very sensitive to small changes in the sample.
- Stiffening and hysteresis in **SA-OSG**: Porous structure and deformation mechanism.
- A **general map** of E/Es vs p has been plotted.
- Effective **CTE** values have been determined for BEoL stack with different Cu line direction and density.
- The Wedge Indentation method delivers robust adhesion measurements without sample preparation.

Acknowledgement

Sven Niese, Yvonne Ritz,
Martin Küttner,
Rüdiger Rosenkranz,
Zhongquan Liao

SRC® Semiconductor Research Corporation

task 2246.001:
"Multi-Scale Materials Database for 3D TSV Stacks – Input for Stress Simulation and Model Validation"

Thank you!


Picture: Fraunhofer IPMS

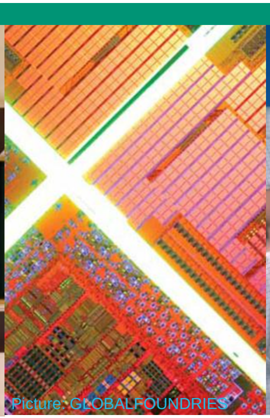
Picture: GLOBALFOUNDRIES

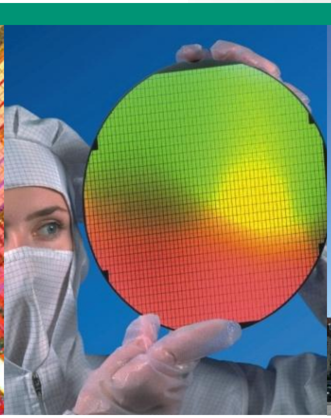

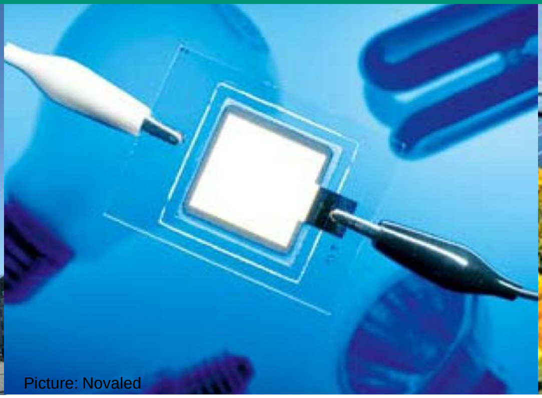
Picture: Novaled

christoph.sander@izfp-d.fraunhofer.de www.izfp-d.fraunhofer.de

Fraunhofer
IZFP